An Investigation of the Viedma Deracemization Process
on Conglomerate Crystals of Achiral Molecules

Dylan Thomas McLaughlin

A Thesis
in
the Department
of
Chemistry and Biochemistry

Presented in Partial Fulfillment of the Requirements
for the Degree of Master of Science (Chemistry) at
Concordia University
Montréal, Québec, Canada
August 2012

CONCORDIA UNIVERSITY

School of Graduate Studies

This is to certify that the thesis prepared

By:

Entitled:

and submitted in partial fulfillment of the requirements for the degree of

Master of Science (Chemistry)

complies with the regulations of the University and meets the accepted standards with respect

to originality and quality.

Signed by the final examining committee:

_____ Chair
Dr. Xavier Ottenwaelder

_____ Examiner
Dr. Yves Gélinas

_____ Examiner
Dr. Pat Forgione

_____ Supervisor
Dr. Louis Cuccia

Approved by _____
Chair of Department or Graduate Program Director

_____ 20___   _____
Dean of Faculty

ABSTRACT

An Investigation of the Viedma Deracemization

Process on Conglomerate Crystals of Achiral Molecules

Dylan Thomas McLaughlin

Viedma deracemization is the attrition-induced asymmetric amplification of a conglomerate crystal mixture of achiral or racemizing compounds. There are 13 reported crystalline systems that undergo Viedma deracemization that can be classified as having: (*i*) achirality in solution, (*ii*) a racemizing state in solution or (*iii*) a reversible racemizing reaction in solution. This phenomenon is based on an autocatalytic attrition-enhanced Ostwald ripening process with a requirement for an achiral, or rapidly racemizing state in solution. The concepts of *'chiral amnesia'*, where a molecule's chiral memory is lost in solution, and *'the common ancestor effect'*, where the chirality of daughter crystals is the same as the mother crystal, can be used to rationalize the generation of a homochiral solid-state. The involvement of chiral clusters in the overall deracemization mechanism is critical. This research explores the generality of Viedma deracemization for an additional 5 achiral organic molecules: benzil, diphenyl disulfide, benzophenone, butylated hydroxytoluene and tetraphenylethylene. Stochastic chiral crystallization was observed for benzil, however chiral crystallization for butylated hydroxytoluene, diphenyl disulfide, tetraphenylethylene and benzophenone was non-stochastic, likely resulting from a cryptochiral environment. Under standard Veidma deracemization conditions, each system reached homochirality within 2 to 30 hours. A shaking mechanism and liquid assisted grinding conditions were also examined and yielded homochiral benzil crystals as little as 10 minutes. Chiral methylbenzylamine was used to direct the chiral amplification of benzil as an example of implementing *'the rule of reversal'* under attrition conditions, where (R)-methylbenzylamine yielded M-form benzil and (S)-methylbenzylamine yielded P-form benzil.

• • •

Acknowledgments

I would like to take the time to thank the amazing individuals who were able to help me get as far as I did. Without your support and help, I would not be where I am now.

<u>To my supervisor</u>,

Dr. *Louis Cuccia*, I want to express my utmost gratefulness for the patience, guidance and support you provided during my tenure as a Masters student. Without you, this thesis would not have been possible and for this I cannot thank you enough. You have been extremely patient with my writing and I am glad to say that I was able to improve with your help. You have shown me skills and qualities that have demonstrated what it means to be a true scientist and you have been an ideal role model for me to follow. You have always been there for me and listened to my problems both inside and outside the lab and I appreciate the help you have given me. I will not forget this experience and I hope we cross paths again in future projects.

<u>To my committee member</u>,

Dr. *Yves Gélinas* and Dr. *Pat Forgione*, I could not ask for better committee members. You have been helpful and supportive during each committee meeting by guiding my project with great suggestions and ideas. This support was also extended outside of meetings and is greatly appreciated. Your advice has helped me overcome many difficulties and made me a better scientist. I thank you again and hope to receive more guidance from you in the future.

<u>To my entire family</u>,

who have been always supportive during my studies away from home. I specifically want to thank my father *Leigh*, my mother *Ginette*, my brother *Myran* and my grand-mother *Helene* for always having faith in me and encouraging me during hard times. Words cannot describe how much I appreciate the love and support you have given me.

● ● ●

<u>To the faculty and staff</u>,

thank you for making my Masters project at Concordia engaging. The atmosphere at Concordia is very similar to Mount Allison University and facilitated the transition when I moved. I had the pleasure of experiencing an open door policy which made talking with you that much easier. I was able to gain new mentors and friends at the same time. I want to specifically thank *Dr. Judith Kornblatt* for the training she gave me on the circular dichroism instrument and *Dr. Rolf Schmidt* for the training, advice and sarcasm he shared with me; I would not trade this for anything in the world. I also would like to thank *Dr. John Capobianco* for the support he has given me during my Masters project and thesis, it is much appreciated and I am truly looking forward to working for you on my Doctorate project. A huge thank you to the staff is required, especially the secretaries, for making our lives easier as graduate students*. Joanne Svendsen*, *Janet Bellefontaine, Maria Ciaramella* and *Hillary Scuffell*, thank you so much for allowing me to lean on you on the rainy days, you do not understand how much help it was and how much I still appreciate it.

<u>To the Supramolecular lab,</u>

thank you for making my experience enjoyable. I really relish our time together whether it was helping each other or simply enjoying each other's company. You made research that much more fun and interesting. I really want to thank *Nadime Salamé* for taking time from his schedule to sit down and help me edit my thesis. It was truly appreciated and this thesis would not be the same without your help. I would also like to thank *Henry Leung*, *Cheng Bian* and *Elliot Goodfellow* for their preliminary work on this project.

<u>To all my friends</u>,

thank you for being there when I was in need of help with a specific task in the lab, understanding a concept, time to cool off after a bad experiment or even just a break after a

long day, you were always there for me. Even though it does not seem like much, you have

helped keep me going when I was down. I could not ask for better friends.

Dedication

This thesis is dedicated to my loving grand-father, *Floyd McLaughlin*, who passed away during the course of this project.

Contents

List of Figures

• • •
x

List of Tables

List of Equations

Abbreviation

1,8-diazabicyclo[5.4.0]undec-7-ene – DBU

Enantiomeric excess - *ee*

1. Introduction

1.1. Chirality in nature

Chirality is a term used to describe the asymmetry of molecules that are mirror images of one another but also non-superimposable (*i.e.* enantiomers). One of the intriguing mysteries in science is why the molecular building blocks of life are almost exclusively of one handedness (*e.g.* L-amino acids and D-sugars).[1-4] This vast dominance of one handedness is unexpected, since the laboratory synthesis of chiral molecules in the absence of chiral auxiliaries, normally results in racemic mixtures (*i.e.* an equal mixture of both enantiomers).[1] Much research has focused on discovering the mechanism(s) behind the evolution towards a homochiral state.[1,2] Many theories of homochirogenesis (*i.e.* the origins of homochirality) are based on biotic or abiotic mirror symmetry breaking events, where the latter are more widely accepted.[2] Overall, homochirogenesis relies on an initial broken mirror symmetry event coupled with asymmetric amplification to a homochiral state.[1-3] Three recognized mechanisms for broken mirror symmetry are: (*i*) parity violation energy difference[5], (*ii*) differential absorption of circularly polarized light[3] and (*iii*) enantioselective adsorption on chiral mineral surfaces.[6] From these processes, a small enantiomeric excess can emerge and, in some cases, be amplified.

An early model used to describe asymmetric amplification from a very small enantiomeric excess was hypothesized by Charles Frank in 1953.[7] He proposed an autocatalysis-mutual antagonism mechanism, where in a pool of substrate and enantiomeric molecules, an enantiomer can interact with the substrate to catalyze a reaction that regenerates itself (*i.e.* an autocatalytic reaction). However, it is also possible that both enantiomers can react with one another to create a mutual antagonistic interaction, which prevents the possibility of the enantiomer to interact with a substrate. A simplified model with only one mutual antagonism event per autocatalytic cycle can be used to represent the chiral amplification of a scalemic

mixture (*i.e.* a non-racemic mixture) (Figure 1). This process is reminiscent of implementing 'the common ancestor effect' as an analogy for chiral amplification.[8] The common ancestor effect is a notion brought forth by Cairns-Smith to describe the emergence of homochirality.[9] Although Frank's 1953 report was theoretical, it laid the groundwork for experimental research into asymmetric amplification, which will be highlighted in this thesis.
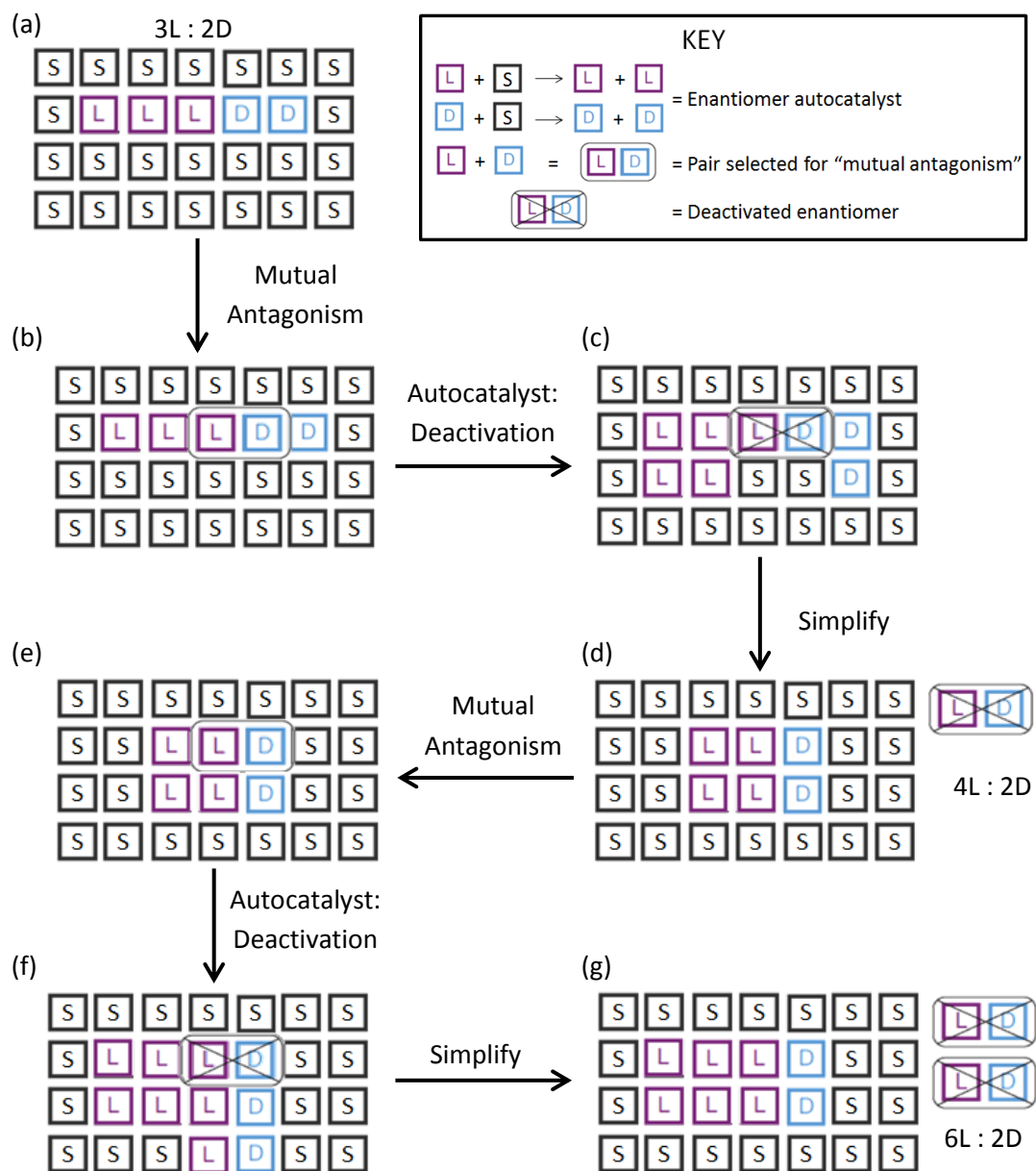
Figure 1. Charles Frank's asymmetric amplification model: **(a)** initial state with 20% enantiomeric excess of L, **(b)** mutual antagonism interaction followed by, **(c)** deactivation and autocatalytic self-replication and **(d)** removal of the deactivated enantiomers from the pool (33% enantiomeric excess of L). **(e, f and g)** the process represented in (b), (c) and (d) is repeated (50% enantiomeric excess of L)

It was not until recently that several experimental examples, following concepts similar to those proposed by Frank, were reported to generate homochiral material.[2] Although the underlying mechanism of homochirogenesis is still not understood, there are now experiments that provide proof that broken mirror symmetry can be amplified to a homochiral state.

• • •

3

Examples include chiral amplification during the sublimation of amino acids,[10] enantioselecitive co-crystallization of amino acids with D- or L- asparagine[11] and attrition-enhanced deracemization of conglomerate crystals, the topic of this thesis.[12]

1.2. Chirality and crystals

The lack of an improper rotation axis, S_n [*N.B.* S_1 = σ (mirror plane) and S_2 = i (inversion center)], is the main method used to identify if a molecule is chiral.[13,14] Chiral molecules are often referred to as optically active due to their ability to rotate the plane of polarized light either clockwise (*dextrorotatory*) or counter-clockwise (*levorotatory*).[15] Although enantiomers have the same molecular formula and physical properties, they behave differently in chiral environments due to their asymmetry. This can be easily visualized with a left hand fitting only into a left-handed glove and a right hand fitting only into a right-handed glove.[1] Indeed, the word chiral originates from the Greek word for hand, χειρ (kheir).[16] Biomolecules are another classic example of the importance of chiral environments. Since chiral biomolecules are almost exclusively homochiral, it is essential to treat enantiomeric molecules, such as chiral pharmaceuticals, as separate entities since they have the potential to interact differently in the body.[17] For example, thalidomide, a drug introduced in the late 1950s to treat morning sickness in pregnant women, is a well-known and tragic example of the importance of chirality (Figure 2).[18] In this case, the (R)-enantiomer is an analgesic, however, the (S)-enantiomer was found to be teratogenic and over 10,000 babies were born with deformities as a result of being prescribed racemic thalidomide.[18] This example establishes the importance of understanding molecular chirality in the pharmaceutical industry. In addition, chirality is equally important in agrochemistry (*e.g.* herbicides, insecticides and fungicides[19]) and food science (*e.g.* flavonoids, amino acids and bioactive amines).[20,21]
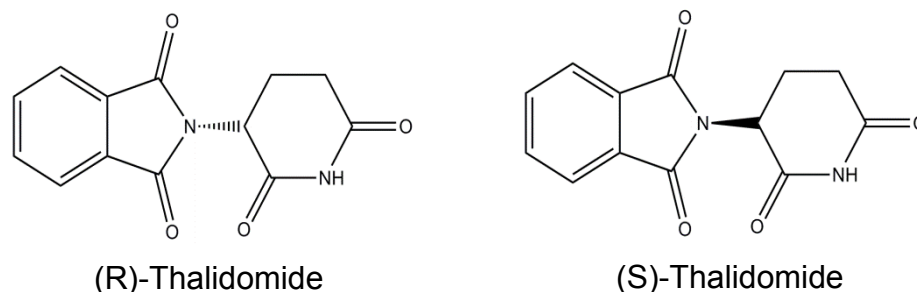
Figure 2. Enantiomers of thalidomide

There are limited routes to prepare (or isolate) enantiomerically pure compounds. Examples include: (*i*) using a chiral auxiliary to synthesize chiral molecules,[22] (*ii*) extracting chiral molecule from a natural source[23] and (*iii*) resolution.[24] More relevant to the topic of this thesis, resolution, "the separation of a racemate into the component enantiomers",[23] typically relies on chiral resolving methods such as chiral chromatography[21] or crystallization.[25]

Crystallization of enantiomers can yield: (*i*) racemic crystals, (*ii*) conglomerate crystals or (*iii*) a solid solution (Figure 3).[25] Racemic crystals have both enantiomers within the unit cell. Conglomerate crystals have only one enantiomer in the unit cell, where both enantiomers crystallize as separate crystals. Solid solutions have both enantiomers in the crystal lattice, however with no regular arrangement.[25] About 90-95% of chiral molecules will crystallize into racemic crystals, whereas 5-10% will crystallized into conglomerate crystals (*N.B.* examples of solid solution crystals are very rare; 0.02%).[13,26]

Racemic Crystals   Conglomerate Crystals   Solid Solution
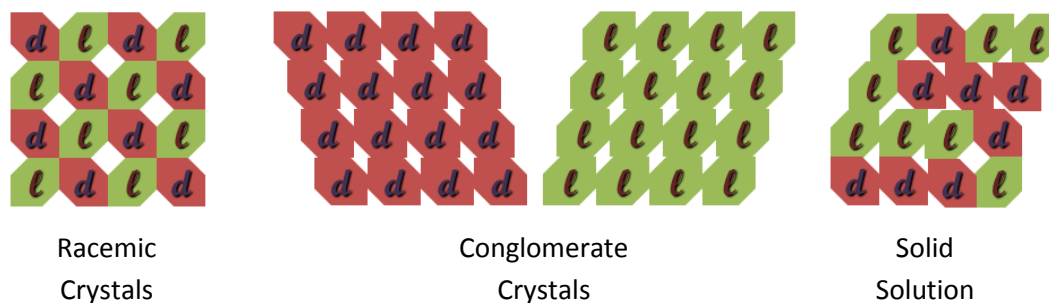
Figure 3. Crystallization of enantiomeric molecules: Racemic crystals have both enantiomers in the lattice, conglomerate crystals are crystals that only have one enantiomer in the lattice and solid solutions are crystals that have both enantiomers present, with no regular arrangement

To separate enantiomers by crystallization, conglomerate crystallization is required. An obvious disadvantage of resolution *via* conglomerate crystallization is that it can only produce a maximum yield of 50%, since only half the racemic material is the desired enantiomer. To overcome this limitation, new approaches have been brought forward and include: (*i*) seed crystallization in a racemizing saturated solution[27] and (*ii*) Viedma deracemization, the main topic of this thesis.[28]

1.3. Achiral molecules to chiral crystals

Chirality is not only observed at the molecular level, but also at the supramolecular level in two-dimensional and three-dimensional assembled structures.[29,30] This supramolecular chirality is due to the ability of molecules to self-assemble into asymmetric structures. Crystallization is the quintessential example of self-assembly,[31] where non-covalent interactions assemble molecules together into an infinite array of repeating packing units called, 'unit cells'.[32]

Crystallization requires a change in the dynamic equilibrium of a solution where the energy is no longer at a minimum. This can be achieved by changing the temperature, pressure, pH or chemical potential of a solution.[33] A steady state supersaturation (or supercooling) is essential to increase the free energy and allow crystals to nucleate and grow.[33] The process of crystallization relies on: (*i*) primary nucleation and (*ii*) secondary nucleation. Primary nucleation is the initial formation of a nucleus by molecules packing together without any external influences.[34] Nucleation occurs when molecules are distributed in a solvent and begin to agglomerate together to create a cluster. In solution, nuclei clusters are unstable until a critical size is reached, where the critical size of a crystal cluster is a function of saturation and temperature of the solution.[33] Secondary nucleation is the growth of a primary nucleus or external nucleus into larger crystals.[34] Crystals grow while keeping the lowest surface energy

possible.[33] The growth rates of various crystal faces differ due to their distinct surface energies and will generate a specific crystal habit (*i.e.* ideal shape of a crystal) and morphology.[34] The different faces on a crystals are assigned using Miller indices [h,k,l].[35] These values represent the reciprocal points where the face would intersect in a Cartesian plane (Figure 4). In addition, a bar over a number represents the negative value ($\bar{1}$ is equivalent to -1).[35] For example, [120] signifies a plane that passes through the Cartesian value of x equal to 1, y equal to 1/2 and z equal to 0.
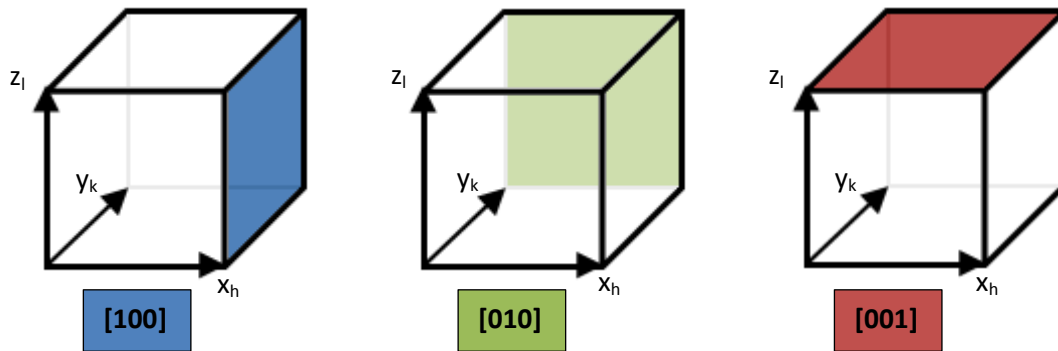
Figure 4. Examples of Miller indices: the blue face is an example of the plane only along the x axis at a value of 1, the green face is an example of the plane only along the y axis at a value of 1 and the red face is an example of the plane only along the z axis at a value of 1

Crystals can be characterized using space groups, a system that describes the packing lattice and translational symmetry operations. There are different nomenclatures used to describe space groups, however, the most commonly used is the Hermann-Mauguin notation [L_{ikj}], where the four letters consist of a Bravais lattice (L) and three translational symmetry operations for the three different direction (*i.e.* i: primary direction, k: secondary direction and j: tertiary direction).[36] In general the Bravais lattices can be separated into four distinct packing lattices, the simplest being the 'primitive' lattice. The primitive lattice (P) has lattice points at each corner of a cube. All other Bravais lattices have the same attributes as the primitive unit cell, with additional lattice points. They are: face-centered lattices (A, B or C), all face-centered

lattice (F) and body-centered lattice (I) (Figure 5A).[37] The translation symmetry operations consist of screw axes and glide planes. A screw axis is described by a rototranslation symmetry element with the rotation defined by 360°/n, where n is the number of rototranslations until the lattice point returns to its original position. The translation between lattice points (before returning to its original position) is given in the form of a fraction of the unit cell as S/n. The term S denotes the amount of translation that has occurred before the rototranslation returns the lattice point to its original position. To simplify the notation when describing a screw axis, it is denoted as n_S to describe both the rototranslation (n) and the translation amount (S) (Figure 5B). Finally, a glide plane is a translation combined with a mirror reflection (Figure 5C).[35]
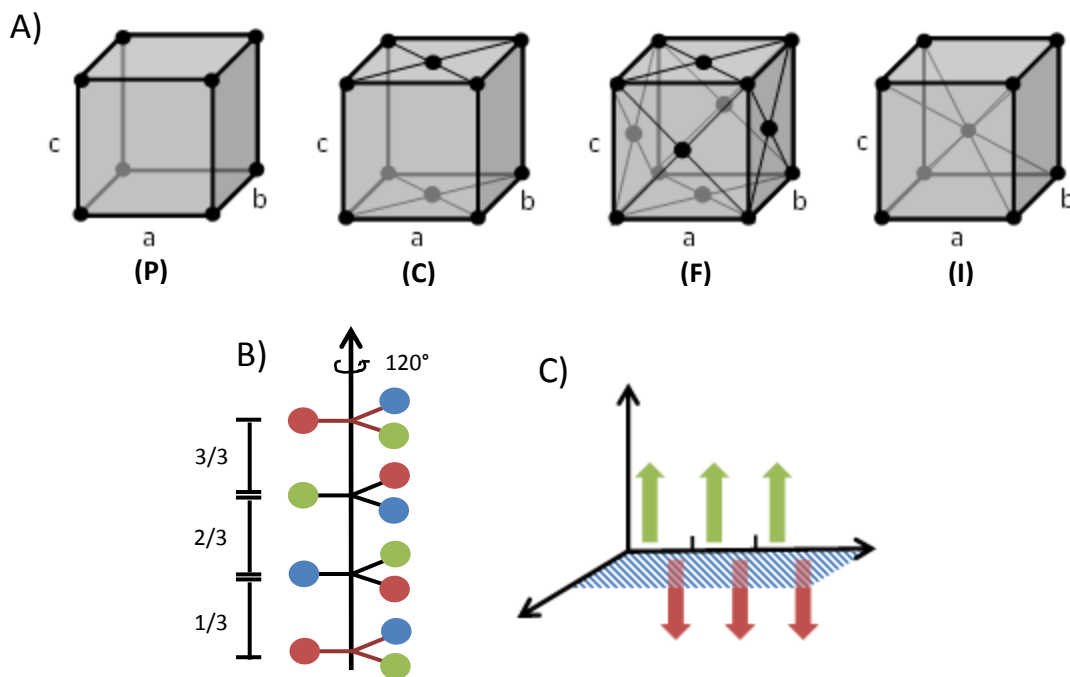
Figure 5. The Bravais lattices, screw axis and glide plane: (A) 4 of the 14 Bravais lattices: (P) Primitive lattice, (C) Face-centered lattice on C face. (F) All face-centered lattice and (I) Body-centered lattice. (B) A 3_1 screw axis where the atoms have a rotation of 120° and is displaced 1/3 in the Z-direction. (C) An example of a c-type glide plane where the arrow are inverted by the mirror pane and translated

Only 230 space groups can be generated when combining all the different possible symmetry operations. Of these 230 space groups, 65 of them are non-centrosymmetric

'Sohncke' space groups and generate chiral crystals.[14,35,38] These 65 space groups are called Sohncke space group since, in 1876, Leonhard Sohncke identified them based on the symmetry operations (the unit cell) without considering the chirality of the packed crystal structure (supramolecular structure).[13,38] It is important to note that only 11 (22 if you include their enantiomorphic partner) of the 65 space groups are actually chiral.[13] The Sohncke space groups can be divided into two categories:[13] (*i*) those with enantiomorphic unit cells (*e.g.* $P3_1$ is enantiomorphic with $P3_2$) which are chiral space groups and *(ii)* those where the unit cell is not enantiomorphic (*e.g.* $P2_1$ and $P2_12_12_1$) which are considered achiral space groups (Table 1). In the latter case, although the unit cell is achiral, there is chirality at the supramolecular level. In terms of space groups, chirality within a crystal is only possible when it lacks glide planes and inversion operations.[39]

Table 1. 65 chiral and achiral Sohncke space groups

Chiral Sohncke space groups <enantiomorph>	Achiral Sohncke space groups
$P4_1$ <$P4_3$>	$I4$
$P4_12_12$ <$P4_32_12$>	$I4_1$
$P4_122$ <$P4_322$>	$P422$
$P3_1$ <$P3_2$>	$P42_12$
$P3_112$ <$P3_212$>	$P4_222$
$P3_121$ <$P3_221$>	$P4_22_12$
$P6_1$ <$P6_5$>	$I422$
$P6_2$ <$P6_4$>	$I4_122$
$P6_122$ <$P6_522$>	$P3$
$P6_222$ <$P6_422$>	$R3$
$P4_132$ <$P4_132$>	$P312$
	$P321$
Achiral Sohncke space groups	$R32$
$P1$	$P6$
$P2$	$P6_3$
$P2_1$	$P622$
$C2$	$P6_322$
$P222$	$P23$
$P222_1$	$F23$
$P2_12_12$	$I23$
$P2_12_12_1$	$P2_13$
$C222_1$	$I2_13$
$C222$	$P432$
$F222$	$P4_232$
$I222$	$F432$
$I2_12_12_1$	$F4_132$
$P4$	$I432$
$P4_2$	$I4_132$

In general, the most commonly observed Sohncke space groups are: $P2_12_12_1$ (orthorhombic crystal structure with a primitive lattice and screw axes in all directions), $P2_1$ (monoclinic crystal structure with a primitive lattice and a screw axis on the primary axis), C2 (monoclinic crystal structure with a face centered lattice and a screw axis on the primary axis) and P1 (triclinic crystal structure with a primitive lattice and a screw axis on the primary axis).[26]

When crystallizing achiral molecules, roughly 8% will crystallize into Sohncke space groups.[40] This can be rationalized using Wallach's rule, where racemic crystals (achiral crystals in this case) are observed to be denser than their chiral counterparts (conglomerate crystals).[41] This observation suggests that a heterochiral crystal packs more efficiently than a homochiral crystal.[41] Chirality is observed in crystals of achiral molecules as a result of locked conformations in the crystal lattice and asymmetric packing. Chiral assembly can be due to: (*i*) axial chirality induced within bonds of a normally achiral molecule or (*ii*) packing achiral molecules in a helical arrangement.[40] Although achiral in solution, crystallization can lock bond rotations of a molecule into an axial chiral conformation in a crystal. Chirality can also be obtained when an achiral molecule packs asymmetrically and generates a helix. When looking at a helix from the top, it will move inwards in either a clockwise or counter-clockwise direction. These chiral helical configurations are known as P (*plus*) or M (*minus*), respectively (Figure 6).

M-Configuration   P-Configuration
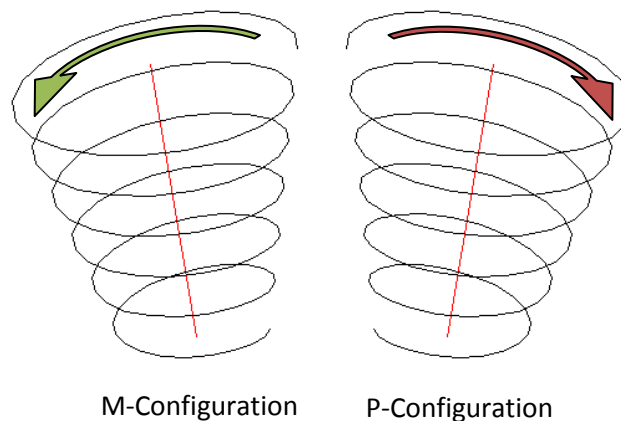
Figure 6. M- and P-form helices: On the left is an example of a left-handed (counterclockwise rotation) helix with M (minus) configuration and on the right is an example of a right-handed (clockwise rotation) helix with P (plus) configuration

1.4. Viedma deracemization

The study of chirality has been closely associated with crystallization since Louis Pasteur first resolved chiral crystals of sodium ammonium tartrate based on the dissymmetry of the

individual crystals.[15] Since then, finding methods of spontaneously generating homochirality in materials has been sought after and intensely investigated.[2]

Kipping and Pope demonstrated another method for obtaining homochiral conglomerate crystals by seeding crystals of sodium chlorate in saturated solutions.[42] Since sodium chlorate is achiral in solution, it can crystallize into either a left- or right-handed chiral conglomerate crystal. Therefore, when the achiral solution is seeded with chiral seed crystals (either left- or right-handed), it continues to grow by secondary nucleation. The growth of the crystal only generates one handedness since it packs with the same configuration as the seed crystals. Kipping and Pope were able to generate homochiral conglomerate crystals by chiral seeding in an achiral solution.

An early example of spontaneously generating one enantiomer of a racemic mixture was demonstrated by Egbert Havinga.[27] He used a chiral ammonium salt, allylethylmethylanilinium iodide, which racemizes quickly in chloroform and crystallizes into conglomerate crystals. The experiment consisted of seeding a saturated solution and allowing it to crystallize over a period of one month at 0 °C. Out of 14 experiments, 12 generated samples that rotated the plane of polarized light. Ideally, once a primary crystal forms in saturated solution, the crystal grows, depleting the crystallizing enantiomer in solution and driving the racemization equilibrium towards the handedness of the crystallizing enantiomer (Figure 7). This results in the crystal growth of one enantiomer and depletion of the other until the chiral molecule has completely crystallized as one enantiomer. In addition, polarimetry showed very little to no rotation of plane-polarized light in the solution phase, as expected. This example demonstrates that by introducing racemization in solution, complete resolution of one enantiomer can be achieved by crystallization (*i.e.* 100% yield is possible).
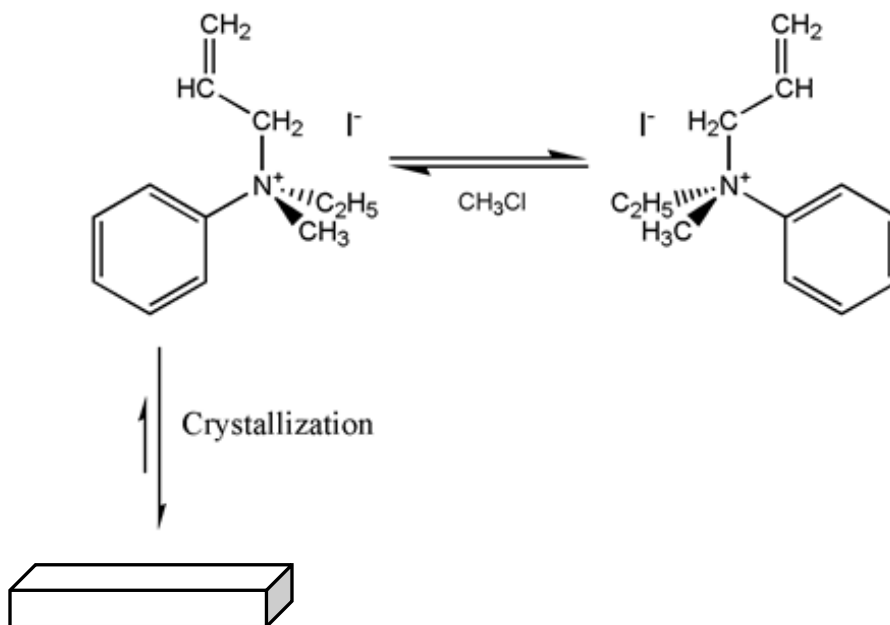
Figure 7. Resolution of enantiomers by racemization and secondary nucleation: Allylethylmethylanilinium iodide racemizes quickly in chloroform and in the presence of a single crystal, growth of a single enantiomer occurs by driving the equilibrium towards the growth of the crystal

Stirred crystallization is another example of a technique that can generate a high enantiomeric excess.[43,44] In 1990, Kondepudi *et al.* demonstrated that stirring an achiral saturated solution of sodium chlorate generated either left-handed or right-handed conglomerate crystals with high enantiomeric excess.[43] This process was also demonstrated with stirring melts of binaphthyl, generating either the R or S enantiomorphic crystals with high enantiomeric excess.[44] The driving force for this process is based on a stochastic primary nucleation event that is subsequently amplified by secondary nucleation (Figure 8). When a saturated solution (or melt) encounters an initial primary nucleation event, through stirring the mother crystal will fragment into daughter crystals. For example, it has been shown that binaphthyl grows into whisker crystals that break very easily at high saturation.[45] These secondary nucleation and fragmentation processes are repeated until crystallization is complete. This results in a high enantiomeric excess and, more often than not, homochirality. Since the solution (or melt) is highly saturated, once a crystal is formed, secondary nucleation is

much more favorable than primary nucleation and there are virtually no further primary nucleation events.[44]
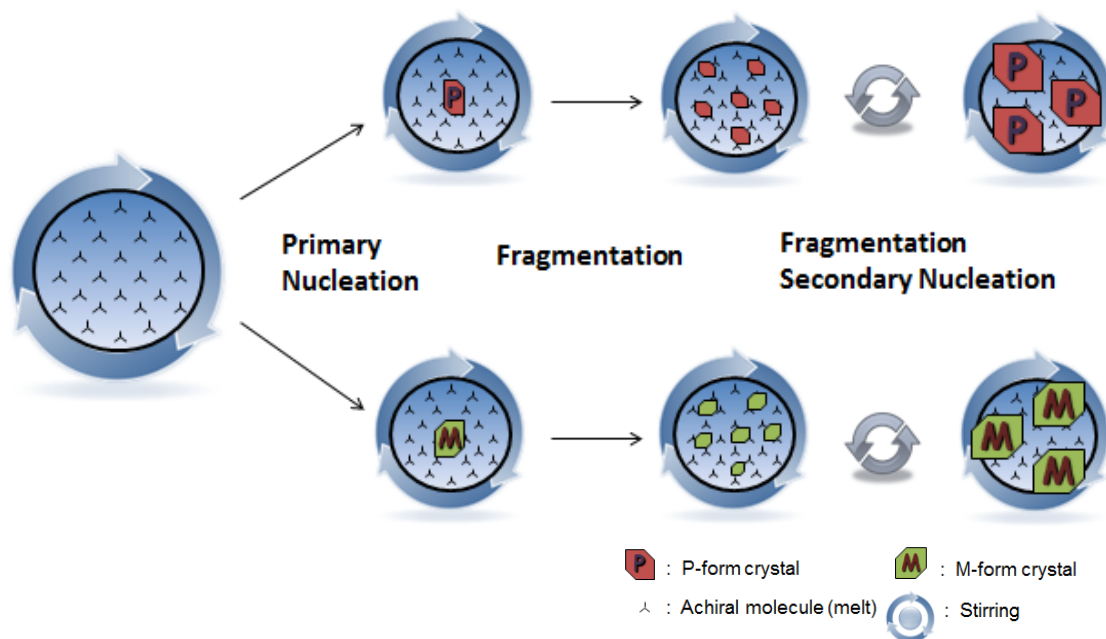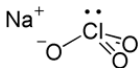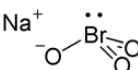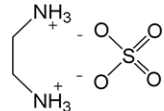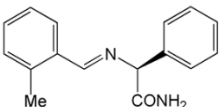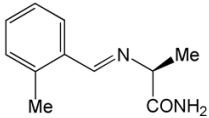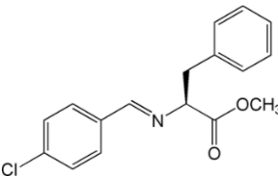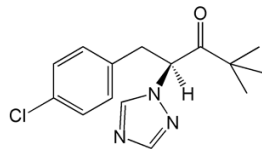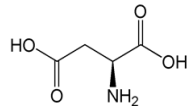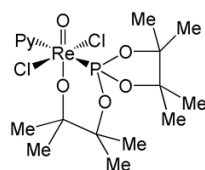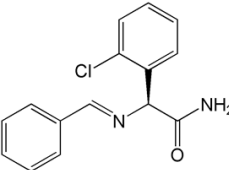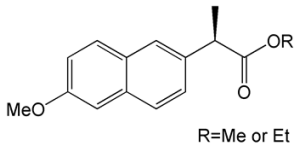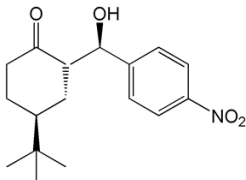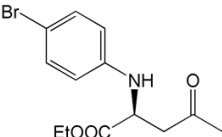
Figure 8. Kondepudi stirred crystallization: The initial event consists of primary nucleation. Through stirring, fragmentation of the mother crystal occurs, breaking into daughter crystals with the same chirality as the mother crystal. The daughter crystals grow through secondary nucleation and undergo fragmentation again from stirring generating new daughter crystals

For the processes described above, spontaneous generation of homochirality originates from a single crystal created by a primary nucleation event or added as a seed, and the system is subsequently overwhelmed by secondary nucleation growth. However, within the past decade, spontaneous generation of homochirality was observed when starting with a racemic mixture of conglomerate crystals. In 2005, Cristóbal Viedma demonstrated that a racemic mixture of sodium chlorate crystals in saturated solution can spontaneously transform to homochirality under attrition conditions (*i.e.* by grinding).[12] This process is now often referred to as 'Viedma deracemization' or 'Viedma ripening'.[46] It is a solid phase transformation that, due to the attrition conditions, yields homochirality in conglomerate crystalline systems when coupled with an Ostwald ripening process.

This simple technique has spawned the interest of many researchers as it provides an unprecedented route for the spontaneous resolution of a racemic mixture. However, many scientists were initially sceptical of this novel process for generating homochiral crystals developed by a relatively unknown geologist in Spain. There are currently 13 examples in the literature that report Viedma deracemization transforming racemic crystal mixtures to homochirality. These include achiral molecular systems, chiral molecular systems (including pharmaceutically relevant compounds), metal complexes, and chiral systems based on reversible reactions (Table 2). Alternative methods to carry out Viedma deracemization are also being explored, and include sonication[47] (instead of stirring with grinding media) as well as simply boiling a saturated solution of a racemic mixture of conglomerate crystals. Since Viedma's initial report in 2005, new molecular systems and technical variations have been investigated to further understand the theoretical aspects of this process as well as to probe the potential for practical applications.

Table 2. Molecules that undergo Viedma deracemization

	Compound	Structure	Compound Type	Reference
A.	Sodium chlorate		Achiral	Viedma Cristobal, *Phys. Rev. Lett.,* **2005** *94*, 065504
B.	Sodium bromate		Achiral	Viedma Cristobal, *Astrobio.,* **2007**, *7(2)*, 312
C.	Ethylenediamonium sulfate		Achiral	Cuccia *et al.*, *Chem. Commun.,* **2008**, 987
D.	Imine of 2-methylbenzaldehyde		Chiral	Blackmond *et al.*, *J. Am. Chem. Soc.,* **2008**, *130*, 1158

Compound		Structure	Compound Type	Reference
E.	Imine of alanine amide		Chiral	Kellogg *et al.*, *CrystEngComm,* **2010**, *12,*
F.	N-(4-chlorobenzylidene)-phenylalanine-methyl		Chiral	Vlieg *et al.*, *Angew. Chem. Int. Ed.* **2008**, *47,* 7226
G.	1-(4-chlorophenyl)-4,4-dimethyl-2-(1H-1,2,4-triazol-1-yl)pentan-3-one		Chiral	Coquerel *et al.*, *Tetrahedron: Asym.,* **2009**,
H.	Aspartic acid		Chiral	Blackmond *et al.*, *J. Am. Chem. Soc.,* **2008**, *130*, 15274
I.	Oxo-rhenium(V) complex		Chiral	Rybak *et al.*, *Tetrahedron: Asym.,* **2008**, *19*, 2234
J.	Clopidogrel (Plavix) precursor		Chiral	Kellogg *et al., Org. Proc. Res. Dev.* **2010**, *14,* 908
K.	Naproxen ester		Chiral	Vleig *et al., Angew. Chem. Int. Ed.,* **2009**, *48,*
L.	Aldol product (4-tert-Butyl-2-[hydroxy-(4-nitro-phenyl)-methyl]-cyclohexanone)		Chiral Reaction	Bolm *et al., Chem. Eur. J.* **2010**, *16,* 3918
M.	Manich product (2-(4-Bromo-phenylamino)-4-oxo-pentanoic acid ethyl ester)		Chiral Reaction	Mauksch *et al., Angew. Chem. Int. Ed.,* **2009**, *48,* 590

1.5.Understanding the Viedma deracemization process

To date, several models of the Viedma deracemization process have been proposed and it is still being investigated actively to fully understand the mechanism.[48-50] There is no complete consensus on the overall mechanism, however there are accepted processes to understand this unexpected transformation of racemic crystals towards homochirality. In this thesis, we will specifically focus on the 'thermodynamic-kinetic feedback near equilibrium' model, first suggested by Viedma.[51,52] The initial theoretical model of Viedma asymmetric amplification was first developed by Uwaha in 2004,[53] and improved in 2008.[50] Noorduin *et al*. later incorporated both models and experimentally demonstrated the theoretical aspects of Uwaha's theories.[52]

The initial model consisted of a continuous attrition, dissolution and recrystallization (Ostwald ripening) cycles that amplify the chirality of the crystals. This is known as the attrition-enhanced Ostwald ripening cycle.[47] A schematic representation of the asymmetric amplification mechanism is given in Figure 8. Attrition breaks up the existing crystals into smaller fragments and according to the Gibbs-Thompson equation, these smaller fragmented crystals dissolve more readily than larger crystals since they have greater surface energy than the larger crystals (*i.e.* the thermodynamic driving force).[51] Fragmentation of the larger crystals also produces new nucleation sites, thus facilitating secondary nucleation-driven crystal growth (*i.e.* the kinetic driving force).[51] The larger crystals grow at the expense of the smaller ones, a well-known process known as Ostwald ripening.[54] This continuous attrition, dissolution and crystallization cycle amplifies any enantiomeric imbalance in the solid phase. Amplification to homochirality relies on 'selective attachment' by chiral recognition between crystals and 'fragmented chiral crystal clusters'.[50]

Coarsening or ripening of a crystal can occur by: (*i*) Ostwald ripening, where larger crystals grow at the expense of smaller crystals, (*ii*) the fusion or attachment of two crystals to

make a new larger crystal or (*iii*) a combination of both Ostwald ripening and crystal attachment.[55] When including this concept in the attrition-enhanced chiral amplification model, it is important to note that homochiral crystal fusion is favored over heterochiral crystal fusion due to chiral recognition.[56] This 'selective attachment' is a necessary coarsening process in the Viedma deracemization process. Due to the collision probability between homochiral crystallites, dissolution of the fragmented crystals lowers compared to a system that has no collision probability.[52] Combining these process mentioned above provides the attrition-enhanced Ostwald ripening mechanism cycle that can be used to explain Viedma deracemization (Figure 9).
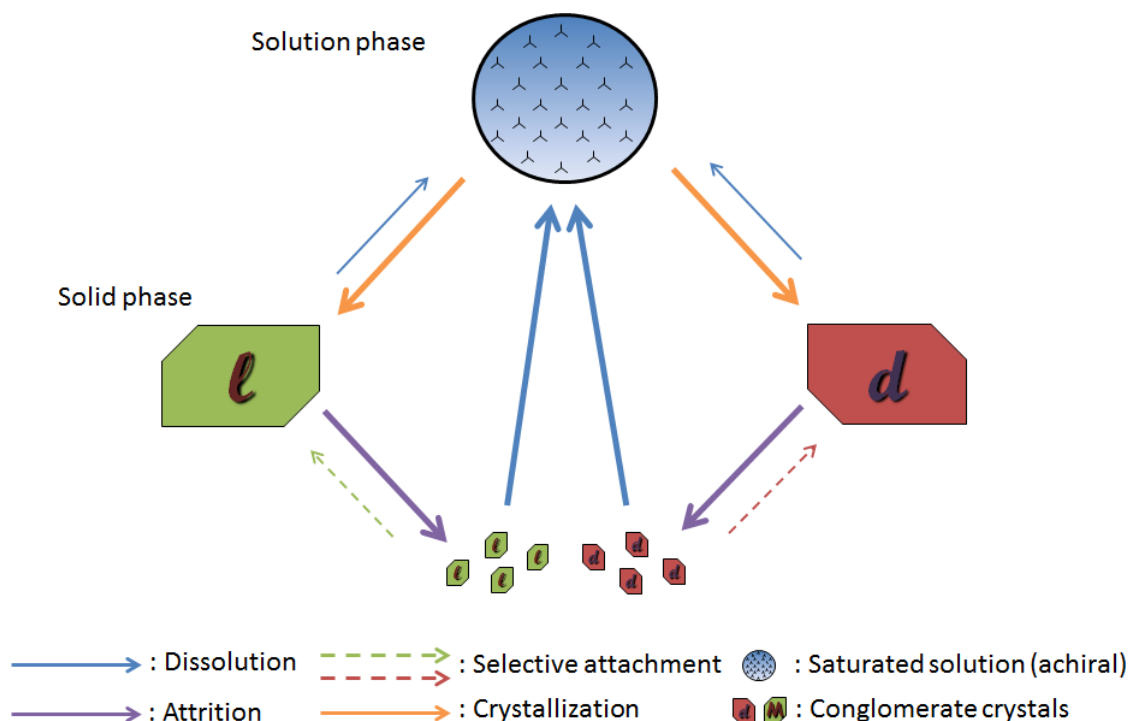
Figure 9. Ideal Attrition-enhanced Ostwald ripening mechanism

There are currently three known driving forces that allow racemic solids to be amplified towards homochirality: (*i*) a common link between conglomerate crystals (achirality or racemization in solution; 'chiral amnesia')[57], (*ii*) crystal size induced solubility[58] and (*iii*) initial chiral imbalances.[52]

Chiral amnesia is a term used to describe how a molecule loses its original chirality during dissolution and recrystallize either on a left- or right-handed crystal.[57] This term describes a 'molecular link' between enantiomorphic crystals. For achiral molecules, chiral amnesia is always present since chirality is lost in solution. In the case of chiral molecules, chiral amnesia occurs when adding a racemization catalyst since interconversion will exist between enantiomers. Without this link, the molecules would dissolve and selectively recrystallize to the same handed crystal with no amplification observed under the Viedma deracemization conditions.[57,58] This link between enantiomorphic crystals is required to observe asymmetric amplification during Viedma deracemization process.[57]

Crystal size-induced solubility is a relatively new driving force used to describe the amplification of racemic conglomerate solids to homochirality.[58] This mechanism is guided by the Gibb-Thompson equation, where smaller crystals have higher solubility.[51] Therefore, under attrition conditions (*i.e.* grinding *via* stirring or sonication), the crystals will fragment to smaller crystallites with increased solubility. The relationship between the crystal size distribution and amplification to homochirality was investigated and reported by Blackmond *et al.*[58] They performed the Viedma deracemization process with Clopidogrel and observed that samples with a larger crystal size distribution did not undergo asymmetric amplification in comparison to those with a smaller crystal size distribution. In addition, they also reported the effects of dynamic dissolution in a saturated solution caused by attrition over a period of time. They observed a normalized value (actual concentration/saturated concentration) of *ca.* 1 until a large seed crystal was added, perturbing the value to *ca.* 0.9 (*i.e.* a drop in concentration) and shifting towards *ca.* 1.05 after 10 minutes of vigorous stirring. The relationship between the crystal size distribution and dissolution denotes an important role in the Viedma deracemization process, since a larger distribution can actually inhibit the amplification process. Additional

evidence of the crystal size-induced solubility as a driving force was demonstrated by inducing different levels of solubility between connected flasks.[58] This was achieved using two flasks connected by circulating solution between them. The initial flask had of a large amount of racemic mixture grinding vigorously (high induced solubility) while the second flask only had a few seed crystals and was gently stirred (low induced solubility). Over time, the initial flask lost its solid phase and the mass was transferred to the second flask. The growth that took place in the second flask maintained the same chirality of the initial seeds. This experiment indicates that material with a smaller crystal size distribution has a higher solubility than material with a larger crystal size distribution. Clearly, a high attrition probability and crystal size distribution have a strong influence on the Viedma deracemization process.

All examples to date show that any initial imbalance will be amplified towards homochirality *via* the Viedma deracemization process. One might question the origin of this initial chiral imbalance or broken mirror symmetry. However, in such crystalline systems, a chiral imbalance can simply occur due to a biased weight ratio, unequal crystal size distribution and/or random fluctuations during the attrition process.[59] For example, when generating a racemic mixture, the mixture can be initially perceived to be 50:50. However, when looking at the molecular level, simple statistics tell us that one enantiomer will dominate very slightly generating a small imbalance.[60] Looking at the example where there are twice as many left-handed crystals (green, *l*) as right-handed crystals (red, *d*) (Figure 10), there is now a higher probability of selective attachment of left-handed fragment crystals. Each cluster has an increased chance of colliding and fusing with homochiral crystallites. Therefore, lowering the overall probability that left-handed fragments will dissolve. In figure 10, each left-handed fragment has two chances out of three to collide with a left-handed crystal, whereas the right-handed clusters only have a one-in-three chance of a favourable encounter. This imbalance

affects the dissolution rate of one handedness over the other, forcing the right-handed crystals to feed the left-handed crystals until homochirality is achieved.[52] This enantiospecific imbalance acts as a driving force to drive chiral amplification in one direction. Viedma deracemization takes advantage of this often unidentified broken symmetry to amplify 'racemic' mixtures to homochirality.
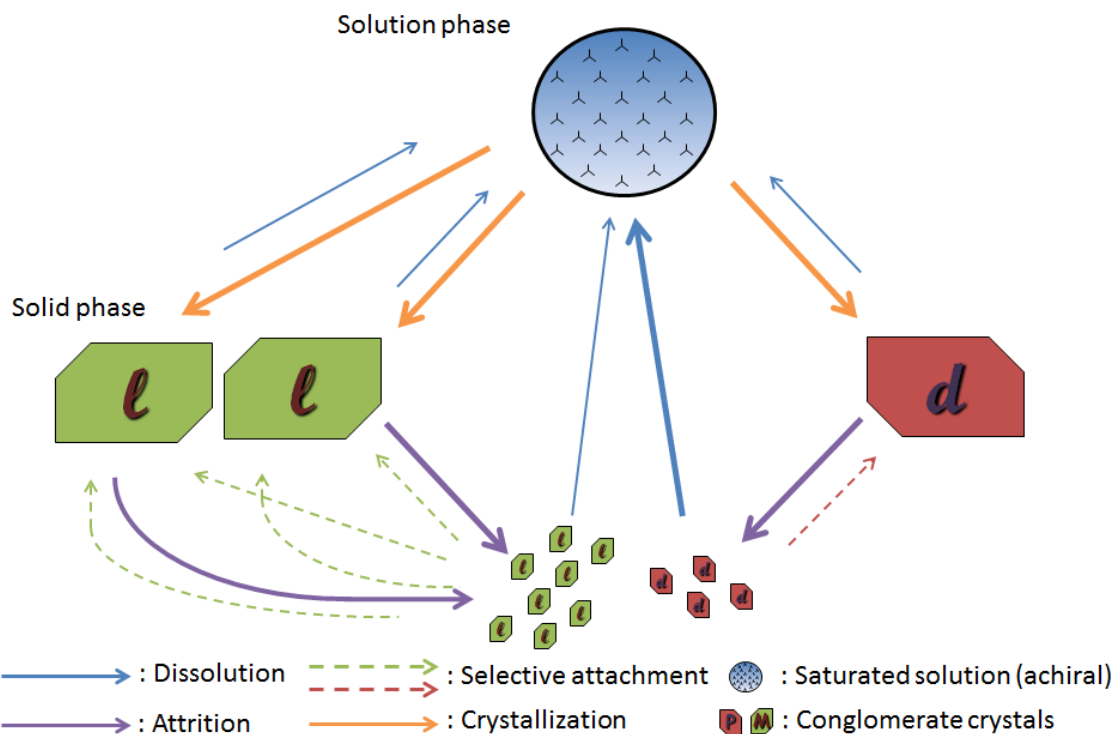
Figure 10. Attrition-enhanced Ostwald ripening mechanism with an enantiomeric imbalance: An increase in the enantiomeric excess lowers the dissolution process since it has a higher chance of selective attachment.

1.5.1. Literature exploration of Viedma deracemization

As stated above, there are currently 13 molecular examples of the Viedma deracemization where a racemic powder was amplified to homochirality. A major goal of this thesis is to further explore the generality of Viedma deracemization. In this sub-section, a literature survey of the different molecules and conditions of the Viedma deracemization process is presented.

Achiral molecular systems are the simplest molecules to undergo Viedma deracemization since the common link (*i.e.* chiral amnesia) between conglomerate enantiomeric crystals is the achiral molecule in solution. When the conglomerate crystals dissolve, the resulting achiral molecules in solution have a 'second chance' to choose a new chirality when crystallizing.[57] There are currently three examples in the literature where achiral molecules undergo Viedma deracemization: (*i*) sodium chlorate (Table 2, A),[12] (*ii*) sodium bromate (Table 2, B)[51] and (*iii*) ethylenediammonium sulfate (Table 2, C).[61] The first example of the Viedma deracemization process was demonstrated with sodium chlorate.[12] Viedma prepared a racemic mixture of left- and right-handed crystals suspended in a saturated aqueous solution with 3 mm glass beads as grinding media. This suspension was stirred at 600 rpm and the crystals were driven to homochirality in *ca.* 24 hours. Viedma also investigated the effect of the amount of grinding media used and the stirring speed on the rate of chiral amplification. He observed that increasing the amount of grinding media and increasing the stirring speed decreased the amplification time. The chiral amplification of sodium bromate crystals in saturated aqueous solution was achieved under similar conditions.[51] Again, an amplification time of *ca.* 24 hours was observed using 4 mm glass beads with a stirring rate of 600 rpm. The latest example of an achiral system to be asymmetrically amplified by the Viedma deracemization process was reported by Cuccia *et al.* using ethylenediammonium sulfate.[61] An amplification time of *ca.* 80 hours was observed when using 0.8 mm ceramic beads with stirring at 2400 rpm. In addition, Cuccia *et al.* also demonstrated that the time to achieve complete chiral amplification was dependant on the stirring rate and the size of the grinding media.

Unlike achiral molecules, chiral molecules require the interconversion of enantiomers in solution in order for Viedma deracemization to take place. The addition of a racemization catalyst, as used in the early spontaneous resolution work described by Havinga,[27] generates a

common link (*i.e.* chiral amnesia) between enantiomers since they are now in equilibrium with one another, similar to the achiral system. Therefore, when a fragmented crystal dissolves, it can racemize in solution and recrystallize to the enantiomorphic conglomerate. There are currently 7 examples of chiral molecules that undergo chiral amplification by Viedma deracemization with racemizing conditions in solution. The first example of a chiral molecule asymmetrically amplifying towards homochirality was an imine of methylbenzyaldehyde (Table 2, D), reported by Blackmond *et al.*[28] Amplification to homochirality for the conglomerate crystals of the imine occurred in a saturated solution of acetonitrile with 5 mol% of 1,8-diazabicyclo[5.4.0]undec-7-ene (DBU) as a racemizing catalyst. Homochiral crystals were obtained in *ca.* 10 days when using 2.5 mm glass beads with stirring at 1250 rpm. Blackmond *et al.* also verified that a small initial enantiomeric imbalance reduces the amount of time required for the chiral amplification process to reach homochirality. Two other imines, an alanine amide (Table 2, E)[62] and phenylalanine-methyl ester (Table 2, F),[63] which both racemize with DBU, also undergo Viedma deracemization. Asymmetric amplification of the imine of the alanine amide was achieved under similar conditions as the imine of methylbenzyaldehyde, however, the authors do not indicate the time required to reach homochirality.[62] Asymmetric amplification of the imine of phenylalanine-methyl ester with 10 mol % of DBU was achieved in *ca.* 4 days using glass beads (unknown size) stirring at 600 rpm.[63] The triazol compound (1-(4-chlorophenyl)-4,4-dimethyl-2-(1,2,4-triazol-1-yl)pentan-3-one) (Table 2, G) in saturated water/methanol (20/80) with 0.7 g of sodium hydroxide as a racemization catalyst, undergoes Viedma deracemization in *ca.* 3 hours using 2 mm glass beads as grinding media with stirring at 700 rpm.[64] Approximately 15 days were required for the Viedma deracemization of aspartic acid (Table 2, H) in saturated acetic acid under racemization conditions with 6 vol.% salicylaldehyde using 2.25 mm glass beads stirring at 1200 rpm at 90 °C.[65] When increasing the temperature to 160°C, an

amplification time of 5 days was observed. In this work, the authors also observed asymmetric amplification under non-attrition boiling conditions. A strong temperature gradient, with a maximum of a 160 °C, produced fast amplification to homochirality in *ca.* 5 days and at 105 °C isothermal heating, amplification was observed but even after 30 days, complete homochirality was not obtained. In this case, the enantiomeric excess in 30 days was *ca.* 60%.

The oxo-rhenium(V) complex (Table 2, I) ([ReOCl$_2$(PO)py] [py = pyridine; PO = (OCMe$_2$CMe$_2$O)POCMe$_2$CMe$_2$O$^{(1-)}$]) is the first example of a metal complex that undergoes Viedma deracemization.[66] There are two enantiomeric *cis* structures for this complex, and they crystallize as conglomerates. In this case, the common link (*i.e.* chiral amnesia) between enantiomers is the *trans* structure, which is accessed by heating the solution. Racemization of the metal complex results from the ability of the pyridyl group to alternate between *cis* and *trans*. Chiral amplification occurred in approximately 9 days when the racemic *cis* product was suspended in saturated boiling toluene and stirred vigorously at 1100 rpm.

The Viedma deracemization process has also been investigated for potential use in industry. This has been highlighted with the chiral amplification of two pharmaceutically relevant molecules. Clopidogrel (Table 2, J), a drug used for treatment of ischemic strokes, heart attacks, atherosclerosis and the prevention of thrombosis, undergoes Viedma deracemization under racemization conditions at the gram scale (approximately 35 g in a volume of 315 mL) using an industrial bead mill.[67] This is the first example of Viedma deracemization on a large scale, highlighting the potential use of this process in the pharmaceutical industry. Here, the minimum time required for chiral amplification was *ca.* 17 hours when grinding at 2500 rpm. A second pharmaceutical compound that was investigated was a Naproxen esters (Table 2, K) (*N.B.* Naproxen is an anti-inflammatory drug).[68] Since

Naproxen crystallizes as a racemic crystal, the Viedma deracemization process was attempted on the conglomerate systems of methyl and ethyl esters of Naproxen. Unlike the systems mentioned above, the Viedma deracemization was also attempted between two enantiomorphic molecules and crystals (methyl and ethyl Naproxen) under esterification and racemization conditions. Both esters were used in this study since a previous investigation of resolving mixtures of methyl Naproxen proved unsuccessful.[68,69] The esterification and racemization process links, by chiral amnesia, all four molecules in solution and allows for crystallization to occur between four crystals (R-methyl, S-methyl, R-ethyl and S-ethyl Naproxen). In addition, this process takes advantage of the solubility, racemization, and reaction properties of both esters. Noorduin et al. started with racemic ethyl ester with a small amount of the (S)-methyl ester and asymmetric amplification towards the (S)-methyl ester was observed. Asymmetric amplification took approximately 5 days when suspended in a mixture of sodium methoxide and methanol (as racemization and esterification conditions) with glass beads (unknown size) stirring at 700 rpm. Since the ethyl ester is more soluble then the methyl ester, it slowly feeds the formation of the methyl ester, driving the formation of the methyl ester crystalline product. In addition, since there was an imbalance of (S)-methyl ester, secondary nucleation drives the formation of crystals with S-handedness.

Aldol[70] and Mannich[71] products (Table 2, L and M, respectively), that crystallize into conglomerate crystals and are obtained by reversible reactions, have also been shown to undergo Viedma deracemization. These two examples are the first of their kind to take advantage of a reversible reaction to interconvert the chiral molecules in solution rather than conventional racemization. The reversible reaction generates two achiral starting materials, which is the racemizing common link, by chiral amnesia, between the chiral enantiomeric products. When the achiral starting materials react to generate a product, either of the

enantiomers is generated (*i.e.* the reversibility of the reaction allows for racemization). The Aldol product undergoes chiral amplification up to 98% enantiomeric excess in 2 to 10 days when starting with an enantiomeric excess of *ca.* 80% to 60%, respectively.[70] This was accomplished by suspending the product in DMSO with 10 mol % of racemization catalyst (pyrrolidine) with ZrO_2 beads (unknown size) and stirring at 800 rpm.[70] The Mannich product amplified to homochirality in *ca.* 7 days in saturated toluene by using a 30 mol % primary amine thiourea catalyst for reversibility and stirring at 1300 rpm with 6 mm glass beads.[71]

Recently, two new molecular systems, sodium ammonium tartrate and threonine, have undergone resolution under attrition-enhanced Ostwald ripening.[58] Blackmond *et al.* confirmed that size induced solubility can be used to resolve enantiomers in the solid phase. They determined that a size-induce solubility gradient between two flasks can occur when vigorous grinding is applied in one flask and gentle grinding in the other. An Ostwald ripening mechanism occurs, through solution transfer, allowing the mass to transfer towards the flask with a lower solubility, induced by gentle grinding.[58] Performing the Viedma process with a racemic mixture allows the solute, with the seed handedness, to transfer in the secondary flask by Ostwald ripening. The overall result was the resolution of the racemic mixture. Blackmond *et al.* were also able to establish that the Viedma deracemization conditions can also be used for the resolution of a racemic mixture without a racemizing agent.[58] It is only fitting that sodium ammonium tartrate, the first example of a racemic mixture resolved by Pasteur himself, can also be resolved under Viedma attrition conditions. In this case, as in a typical resolution, the maximum yield is 50% for each enantiomer.

In a period of less than 10 years, there are only 13 examples of Viedma deracemization (15 when including the resolution method; sodium ammonium tartrate and theorine), the

majority of which are chiral conglomerate crystal systems that require racemizing conditions in solution for chiral amplification. Surprisingly, given the relative abundance of achiral conglomerate crystal systems, sodium chlorate, sodium bromate and ethylenediammonium sulfate are the only three examples demonstrated to undergo Viedma deracemization. These systems can be considered as the simplest, given that the molecules are inherently achiral in solution. The central goal of this thesis is to identify additional achiral conglomerate crystal systems and to explore the scope and generality of the Viedma deracemization process between them.

1.6. Viedma deracemization and mechanochemistry

Viedma deracemization is a solid-state transformation from a racemic mixture to a homochiral mixture driven by attrition. The process can be considered to fall within the realm of mechanochemistry. Mechanochemistry is the study of changing matter under solid-state grinding.[72] Investigations using mechanochemistry have successfully yielded: (*i*) covalent bond formation,[73] (*ii*) coordination bond formation,[74] and supramolecular assembly.[72] In most cases, mechanochemistry can simplify the formation of functional solids and simplify reaction times and methods.[75] It can either be carried out without solvent (neat) or under liquid assisted conditions using a small amount of solvent. To investigate the role of solvent in mechanochemistry, an η parameter (Equation 1) was establish.[76] An η value above 12 μL mg^{-1} is considered to be under solution synthesis, a value between 2 and 12 μL mg^{-1} is considered to be a slurry and a value between 0 and 2 μL mg^{-1} is considered to be liquid assisted grinding.[72] In most cases, Viedma deracemization experiments fall between liquid assisted grinding and slurry conditions (η values of *ca.* 0.5 to 4 μL mg^{-1}).[51,61,70,72]

$$\eta = \frac{Volume\ (\mu L)}{Solid\ powder\ (mg)} \qquad \text{(Equation 1)}$$

Liquid assisted grinding is a relatively new method used in mechanochemistry consisting of using very small amounts of solvent during a grinding experiment (η values of *ca.* 0.1 and 2 µL mg^{-1}).[76] The liquid assisted grinding method was introduced in 2002, where Jones *et al.* investigated "solvent-drop grinding" in the mechanosynthesis of cyclohexane-1,3,5-tricarboxylic acid co-crystals.[77] Liquid assisted grinding experiments are now used to investigate the screening of co-crystals[76] and salts[78] as well as for the synthesis of metal organic frameworks.[79] It is believed that the liquid is either acting as a lubricant during grinding, as a catalyst to help drive a reaction towards a product or it may have an unknown effect during grinding.[72,75] Since the liquid assisted grinding method is relatively new, there are no general explanations for the role of the liquid phase, and it may vary from system to system. Herein, the role of a saturated solution in terms of the η parameter in relation to Viedma deracemization is investigated.

1.7. Directed chiral amplification

1.7.1. By enantioselective adsorption

Adsorption of chiral molecules on chiral surfaces is of exquisite interest since some researchers believe it to be associated with the origin of homochirality in biomolecules.[80] This is a possibility considering that many chiral minerals (*e.g.* quartz) and achiral minerals with chiral surfaces (*e.g.* gypsum and calcite) were present in abundance during prebiotic time. In addition, it has been shown that these minerals can enantioselectively adsorb chiral amino acids on their chiral surfaces. For example, 1.4 ± 0.4% enantiomeric excess was obtained when adsorbing D- and L-alanine on the surface of levorotatory and dextrorotatory quartz, respectively.[80] Enantioselective adsorption of 28 chiral organic molecules, including amino acids, was observed on specific chiral surfaces of gypsum.[80] Enantioselective adsorption of D- and L- aspartic acid

was investigated on the chiral faces of calcite. By dipping calcite crystals in a racemic solution of

D- and L-aspartic acid, enantiomeric enrichments of *ca.* 10% were obtained on specific chiral

faces.[81]

At least three non-linear contact points are required for any chiral material to selectively

bind on a chiral surface (Figure 11).[80] Three non-equivalent interacting groups arranged in a

non-linear fashion will adsorb preferentially on one surface over the enantiomorphic surface, as

seen in Figure 11.[82]
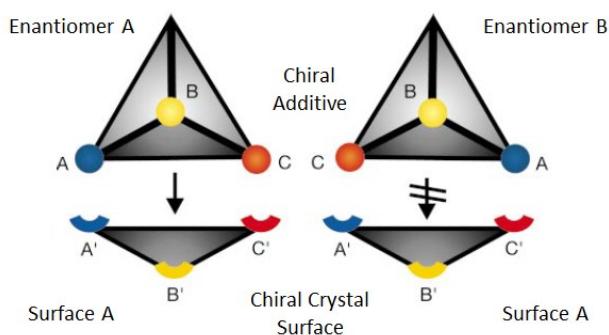
Figure 11. The three point contact model of a chiral enantiomer interacting with a chiral surface:
Generic model of enantiomers adsorbing on the same chiral surface (adapted from ref. 83 with
permission)

Enantioselective adsorption can occur on different chiral faces of a crystal. This effect

has been reported for (R or S)-3-methylcyclohexanone on chiral surfaces of copper by Gellman

et al.[83] An experimental desorption difference of approximately 0.7 ± 0.2 kJ/mol was observed

between specific chiral surfaces and both enantiomers of 3-methylcyclohexanone.   Crystal

growth is also affected when chiral molecules enantioselectively adsorb on crystal surfaces.

Surface analysis (by AFM) of untreated and treated calcite with L- and D-aspartic acid confirmed

an enantioselective change in crystal growth (Figure 12).[80,84]   When untreated, symmetric

growth steps were observed (Figure 12, A), but when submerged in either L- or D-aspartic acid,

enantiomorphic growth steps were observed and believed to be caused by inhibiting growth at certain sites (Figure 12, B).

Untreated Calcite   L-aspartic Acid   D-aspartic Acid
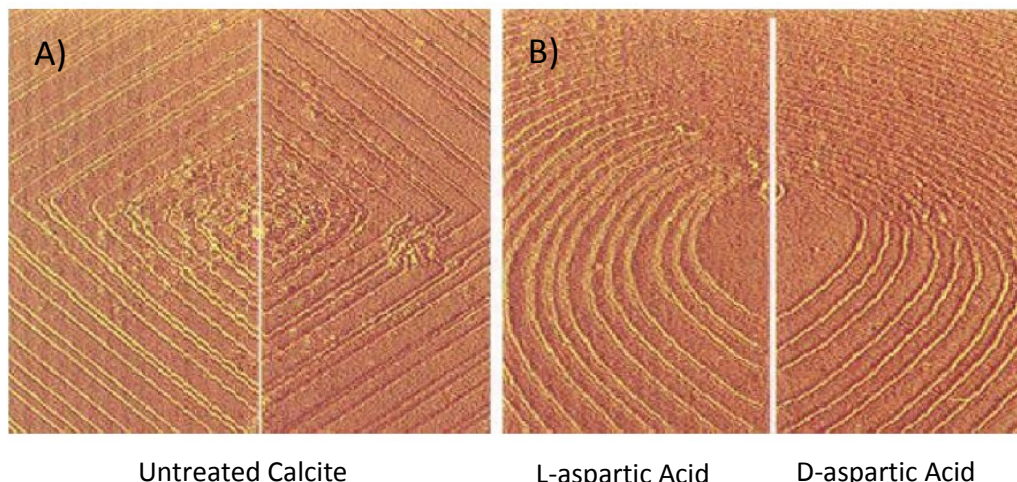
Figure 12. Growth of calcite under treated and untreated conditions: (A) Untreated calcite (B) Treated with aspartic acid (adapted from ref. 81 with permission)

There are some examples of chiral molecules, mainly amino acids, which have been used to direct the asymmetric amplification of Viedma deracemization.[28,62,85,86] Cuccia *et al.* demonstrated the first achiral molecular system (ethylenediammonium sulphate, EDS), that crystallizes into conglomerate chiral crystals, that can be directed using L- and D-amino acids.[85] They categorized their findings into three different groups of amino acids: (*i*) for 13 amino acids, the L-isomers amplified the chirality of EDS towards levorotatory crystals and the D-isomers amplified the chirality of EDS towards dextrorotatory crystals, (*ii*) for 3 amino acids, the L-isomers amplified the chirality of EDS towards dextrorotatory crystals and D-isomers amplified the chirality of EDS towards levorotatory crystals and (*iii*) for 3 amino acids, no directing properties were observed. The initial experiment in directing the asymmetric amplification of a chiral system was explored by Blackmond *et al.* using the imine of methylbenzaldehyde.[28] They demonstrated that (R)-phenylglycine amplified the racemic mixture towards the (S)-methylbenzaldehyde and (S)-phenylglycine amplified the racemic mixture towards the (R)-

methylbenzaldehyde. Blackmond *et al.* also demonstrated that the amplification of an imine of methylbenzaldehyde can be directed by a phenylglycine amide additive.[86] The (R)-phenylglycine amide additive amplified the racemic mixture towards the (S)-methylbenzaldehyde and the (S)-phenylglycine amide additive amplified the racemic mixture towards the (R)-methylbenzaldehyde. Kellogg *et al*. also demonstrated the directed chiral amplification of the imine of methylbenzaldehyde using an alanine additive.[62] (R)-alanine directed the amplification towards the (S)-imine of methylbenzaldehyde and (S)-alanine directed the amplification towards the (R)-imine.

It is thought that a chiral molecule can adsorb enantioselectively on the surface of a chiral crystal and possibly inhibit its growth, allowing the enantiomorphic crystal to grow more rapidly. This is, in essence, the implementation of the 'rule of reversal', a theory developed by Addadi *et al.*[87] The rule of reversal describes the preferential adsorption of a chiral additive to crystals causing a decrease in crystal growth of one enantiomorph, allowing for preferential crystallization of the opposite enantiomorph. The conglomerate systems Addadi *et al.* investigated were (R or S)-glutamic acid hydrochloride, (R or S)-threonine, (R or S)-(*p*-hydroxyphenyl)glycine *p*-toluenesulfonate, and (R or S)-asparagine hydrate, where a series of chiral amino acid additives were shown to induce preferential crystallization. During crystallization, an enantiopure amino acid additive was added to the conglomerate systems, and only one handedness was observed during crystallization. The crystal with additive associated with it grows more slowly and does not reach the critical radius size in solution and redissolves easily, while the crystal not associated with the chiral additive undergoes growth *via* secondary nucleation. Overall, a crystal growth reversal is observed. This early work provides excellent precedence for the ability to direct chiral amplification under Viedma deracemization conditions using chiral additives (Figure 13).
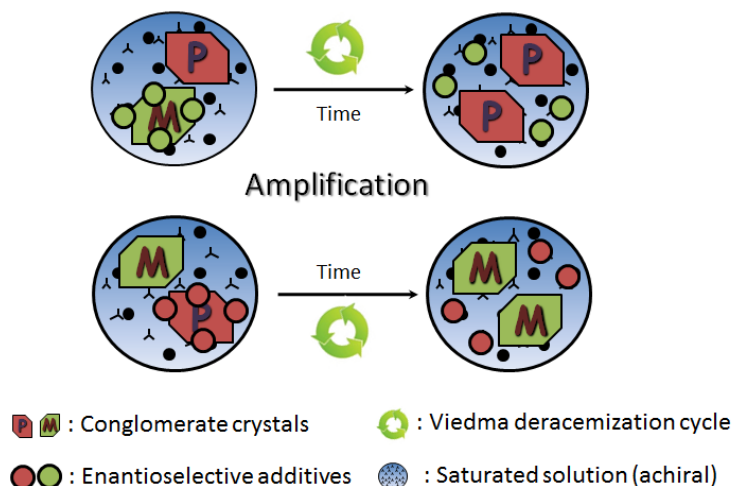
Figure 13. Directed asymmetric amplification using chiral additives

1.7.2. By circularly polarized light

Circularly polarized light has also been regarded to be connected with the origin of homochirality in biomolecules.[3] This is due to the asymmetric photochemical induction that can occur when chiral molecules are synthesized, generating an enantiomeric excess.[3] Scientist strongly believe that circularly polarized light can affect the synthesis of molecules since meteorites that have been exposed with cosmic circularly polarized light have generated amino acids with slight enantiomeric excess.[3]

Circularly polarized light has recently been used to direct the asymmetric amplification of Viedma deracemization. Directed asymmetric amplification is observed since enantiomorphic molecules will differentially absorb circularly polarize light at certain wavelengths.[88] Asymmetric amplification by the Viedma deracemization process will act in accordance to Addadi's rule of reversal, where the non-excited molecule is amplified to homochirality. In this case, it is believed that the excited enantiomorphic molecule crystallizes slowly in comparison to the non-excited enantiomorphic molecule.[88] Vlieg *et al.* demonstrated that exciting the imine of methylbenzaldehyde with circularly polarized light directed the asymmetric amplification:

exciting with *l*-circularly polarized light amplified the (S)-imine of methylbenzaldehyde, and exciting with *d* circularly polarized light amplified the (R)-imine of methylbenzaldehyde.[88]

1.8. Cryptochiral environment
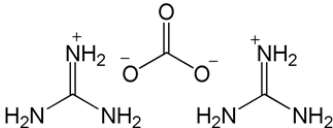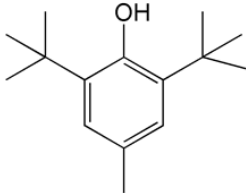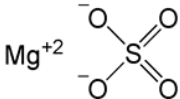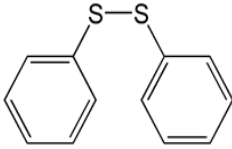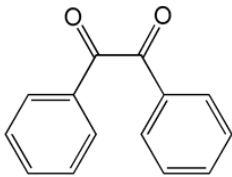
Cryptochiral environments are an elusive source of chiral imbalances. The term 'crypto' originates from the Greek word κρυπτός meaning hidden or secret.[89] In chemistry, the term cryptochiral is defined by a system (or environment) that has optically active material at concentrations not detectable by instruments.[59] Unlike physical imbalances (*e.g.* enantiomeric imbalance by weight ratio), a cryptochiral environment can affect crystallization or even the Viedma deracemization process in the same way as described for the 'rule of reversal'.[28,87]
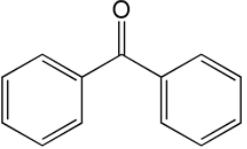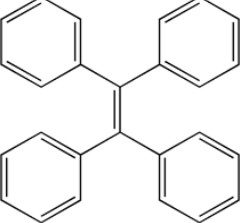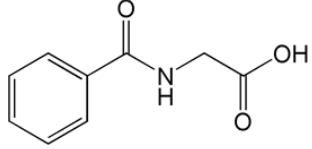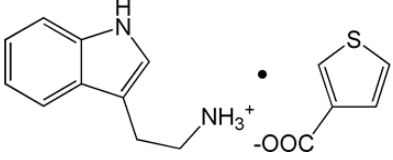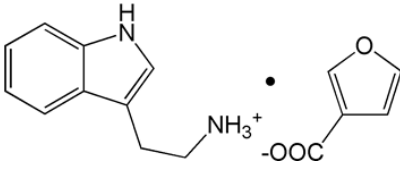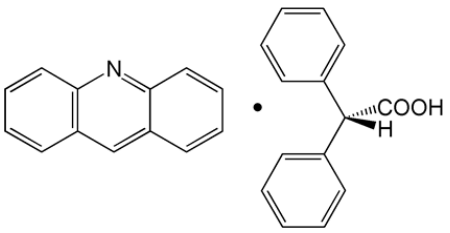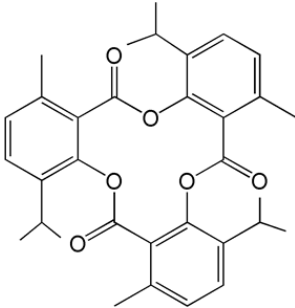
It is tremendously difficult to completely eliminate possible cryptochiral molecules in a world contaminated with chirality.[90] It has been suggested that chiral contamination can also come from the experimenters themselves.[91] An example of this is the conglomerate crystallization of D- and L-tartaric acid copper complexes. When performing the experiment, three different Japanese laboratories were only able to obtain the dextrorotatory crystals. The phenomenon was believed to have been caused by cryptochiral seeding by the experimenters.[90] Cryptochiral seeding can occur from optically active dust particles that are found in various sources.[91] The seed behaves as a nucleus and preferentially favors the growth of one crystal over the other. Some examples of experiments that have possibly been influenced by cryptochiral environments are the crystallization of helical triallylamine copper chloride where only M-form crystals formed,[92] and the crystallization of sodium chlorate, where a series of crystallization generated high ratios of left- *vs.* right-handed crystals (ranging from 60% to 99% in favour of left-handed crystals).[59]
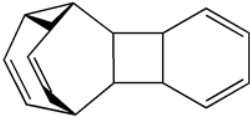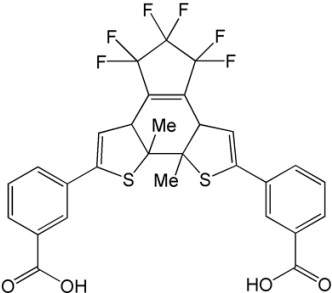
1.9. Thesis objectives

Our initial objective is to investigate the generality of Viedma deracemization on novel systems of conglomerate chiral crystals and to extend this process to purely organic molecules. These systems range from achiral and dynamically racemic molecules, chiral co-crystals, enantiomeric atropisomers and valence isomers. Table 3 lists the compounds that Cuccia's lab is currently investigating. The molecules under investigation in this thesis are benzil, diphenyl disulfide, benzophenone, butylated hydroxytoluene, and tetraphenlylethylene.

Table 3. Molecules that are being investigated for the Viedma deracemization process

Compound	Structure	Compound Type
Guanidine carbonate		Achiral
Butylated hydroxytoluene		Achiral
Magnesium sulfate		Achiral
Diphenyl disulfide		Achiral
Benzil		Achiral

Compound	Structure	Compound Type
Benzopheneone		Achiral
Tetraphenylethylene		Achiral
Hippuric acid		Achiral
Tryptamine • thiophene-2-carboxylic acid		Co-crystal
Tryptamine • 2-furoic acid		Co-crystal
Acridine • diphenylacetic acid		Co-crystal
Tri-*o*-thymotide		Atropisomer

Compound	Structure	Compound Type
Clyclooctatetraene dimer		Valence isomer
Diarylethene derivative (benzoic acid)		Valence isomer

Our secondary objective is to investigate different conditions for Viedma deracemization. This includes exploring alternate attrition conditions and exploring the effect of changing the amount of solvent used. A new Viedma deracemization method by shaking, rather than stirring, using benzil will also be reported. Optimization of this new method and new protocol using a very small amount of saturated solvent (liquid assisted grinding) will be discussed. A long term goal is to explore the possibility of carrying out Viedma deracemization without solvent under attrition/sublimation conditions.

Our third objective is to investigate the potential for directing the chirality during the Viedma deracemization process using chiral additives. If chiral additives have directing capabilities, further experimental and theoretical studies will be carried out to understand the enantioselective binding of chiral additives at chiral crystal surfaces. Directed asymmetric amplification of benzil using an organic chiral additive will be discussed.

1.10. Molecules under investigation

Benzil

Benzil (diphenylethanedione) is an achiral molecule that crystallizes into conglomerate chiral crystals.[40] Benzil is commonly studied due to its photochemical properties [93] and has been used in photographic materials as well as a photoinitiator in radical polymerization.[94] Benzil is a uniaxial class crystal, and has an tetragonal crystal structure belonging to the non-centrosymmetric Sohncke space group, $P3_121$ (BENZIL02).[95]

Diphenyl Disulfide

Diphenyl disulfide (phenyldisulfide) is an achiral molecule that crystallizes into conglomerate chiral crystals.[40] Diphenyl disulfide is commonly studied to investigate the conformations of diphenyl dichalcogenides.[96] Diphenyl disulfide is a biaxial class crystal, and has an orthorombic crystal structure belonging to the non-centrosymmetric Sohncke space group, $P2_12_12_1$ (PHENSS11).[97]

Benzophenone

Benzophenone is an achiral molecule that crystallizes into conglomerate crystals.[40] Benzophenone is commonly investigated due to its crystalline optical activity.[98,99] Benzophenone is a biaxial class crystal and has an orthorombic crystal structure belonging to the non-centrosymmetric Sohncke space group, $P2_12_12_1$ (BPHENO10).[100]

Butylated hydroxytoluene

Butylated hydroxytoluene (2,6-di-*tert*-butyl-4-methylphenol) is an achiral molecule that crystallizes into conglomerate chiral crystals.[40] Butylated hydroxytoluene is most commonly investigated as an antioxidant.[101] Butylated hydroxytoluene is a biaxial class crystal and has an orthorombic crystal structure belonging to the non-centrosymmetric Sohncke space group, $P2_12_12_1$ (MBPHOL02).[102]

Tetraphenylethylene

Tetraphenylethylene is an achiral molecule that crystallizes into conglomerate crystals.[40] Tetraphenylethylene is commonly studied to take advantage of its rich electrochemical and excited state properties.[103] Tetraphenylethylene is a biaxial class crystal, and has an monoclinic crystal structure belonging to the non-centrosymmetric Sohncke space group, $P2_1$ (TPHETY02).[104]

2. Materials and method

2.1. Chemicals

Diphenyl disulfide ([CAS 882-33]; $C_6H_5SSC_6H_5$; F.W. 218.34), benzil ([CAS 134-81-6]; $C_6H_5COCOC_6H_5$; F.W. 210.23), 1,1,2,2-tetraphenylethylene ([CAS 632-51-9]; $(C_6H_5)_2CC(C_6H_5)_2$; F.W. 332.44), butylated hydroxytoluene ([CAS 128-37-0]; $[(CH_3)_3C]_2C_6H_2(CH_3)OH$; F.W. 220.35), xylene ([CAS 1330-20-7]; reagent grade; $C_6H_4(CH_3)_2$; F.W. 106.17) anhydrous toluene ([CAS 108-88-3]; $C_6H_5(CH_3)$; F.W. 92.14) and potassium bromide ([CAS 7758-02-3]; KBr; F.W. 119.00 heated to 440 °C and oven dried at 130 °C]) were purchased from Sigma Aldrich. Benzophenone ([CAS 119-61-9]; $(C_6H_5)_2CO$; F.W. 182.22) was from Anachemia Science. Ethanol ([CAS 64-17-5]; CH_3CH_2OH; F.W. 46.0) was obtained from Commercial Alcohol Inc. Nujol mineral oil ([CAS 8012-95-1] was obtained from Plough Inc.

2.2. Instrumentation

Circular dichroism spectra were recorded using a Jasco J-710 spectropolarimeter. A Mettler Toledo MX5 microbalance was used to prepare samples for circular dichroism. A SPECAC manual hydraulic press with 13 mm evacuable die with two hardened stainless steel pellets was used to prepare KBr pellets. A 1.00 mL glass syringe (SGE Analytical Science) was used for the measurements of solubility. A home-built magnetic stirrer based on a PINE 101 industrial drive (coupled with a PINE MSRX speed control) or a FastPrep®-24 shaker operating at a speed of 5 m/s, (MP bio) were used for Viedma deracemization. YTZ® high wear resistant zirconia grinding media (0.8 mm dia.) were used as the grinding media for Viedma deracemization. A Nikon SMZ1500 microscope coupled with a Nikon DS F1 camera was used to photograph the crystals. SHAPE V7.2 software was used to model and index the prominent faces of each crystal.

2.3.General procedures

2.3.1. Conglomerate crystallization

A predetermined amount of the desired molecule in the required solvent was dissolved

by heating the solution to boiling in a crystallization dish (500 mL; *ca.* 10 cm diameter). The

solution was allowed to cool to room temperature and a watch glass was then placed on top of

the crystallization dish to allow for slow undisturbed crystallization. Crystals were typically

obtained within 4 to 14 days, collected with tweezers and the residual mother liquor was wiped

off each crystal with a Kimwipe. Counting the ratio of left- to right-handed crystal was

accomplished using circular dichroism spectra. The statistics for each system was calculated

using the binomial function in excel (BINOM.DIST(number of outcomes, number of events (N),

probability, FALSE [Probability mass function]).

2.3.2. Visualizing crystal morphologies

An adequate single crystal from each molecular system was picked out of a

crystallization dish for imaging. Crystallographic data of each crystal system was downloaded

from the Cambridge Crystallographic Data Centre (CCDC) and analyzed with in the SHAPE

software. Modeling of the faces was carried out by using the resizing tool and optimizing the

faces until it resembled the representative crystal.

2.3.3. Stirred melt crystallization

In a vial (20 mL), the desired molecule, with a stir bar (3mm x 13 mm; straight), was

heated until it was completely melted. The melt was stirred at 1300 RPM (OtpiChem: Digital

hotplate stirrer) and, with the heating turned off, allowed to slowly cool to room temperature.

The resulting solid was then crushed into a powder using a mortar and pestle. Some samples

were seeded to control the generation of either left- or right-handed samples. The melts were

seeded with *ca.* 10 to 30 mg of crystals with the desired handedness. The seed powder was added when the thermostat reached 1°C below the melting point.

2.3.4. Solubility measurements

In a vial (20 mL), the desired molecule, with a stir bar (3 mm x 13 mm; straight), was slowly dissolved with the desired solvent described in section 2.3.11-2.3.15. The vial was placed in an oil bath at room temperature. The dissolution process was accomplished by adding small increments of solvent using a 1.00 mL glass syringe until the powder was completely dissolved.

2.3.5. Circular dichroism

Circular dichroism (JASCO Corp., J-715) was used as a method to determine the chirality of chiral solid samples. Typical circular dichroism parameters were: 450 to 250 nm with a standard sensitivity, continuous scanning mode, 1 nm bandwidth, 0.2 nm data pitch, 1 sec response, 50 nm/min scan speed and 3 to 5 accumulations. Spectra were collected at room temperature. Circular dichroism spectra were recorded as a Nujol mull between quartz windows (1.05 cm diameter; 0.3 cm thick) or as a KBr pellet (13 mm) as indicated in section 2.3.11-15 and the figure captions.

KBr pellets were prepared by grinding together the desired molecule (described in the sections 2.3.11 to 2.3.15) with potassium bromide using a mortar and pestle. Once the mixture was homogeneous, a portion of the powder was weighed (50 mg) and pressed using a manual hydraulic press (Specac). The weighed powder was placed between two 13 mm pellets and pressed at approximately 8 tons for about 20 seconds. The pellets was then placed in a homemade cardboard holder and positioned in the spectropolarimeter for analysis.

Nujol mulls were prepared by grinding together the desired molecule (described in section 2.3.11) with Nujol mineral oil using a mortar and pestle. Once the mixture was

homogenous, a portion of the oily mixture was weighed (10 mg) directly on a quartz plate (1.05 cm diameter; 0.3 cm thick). A second quartz plate was used to sandwich the mixture. The quartz/Nujol sample assembly was then placed in a homemade holder and positioned in the circular dichroism spectropolarimeter for analysis.

2.3.6. Enantiomeric excess calibration curve

A calibration curve was generated using a constant weight with different ratios of left-handed and right-handed single crystals of the desired molecule (described in section 2.3.10-14). The enantiomeric excess was calculated using Equation 2. In Equation 2, x_l is the weight of left-handed crystal and x_d is the weight of right-handed crystals. The samples were analyzed based on different enantiomeric excess ratios. A calibration curve was generated by plotting the circular dichroism signal versus enantiomeric excess. The enantiomeric excess of unknown samples was determined using this calibration curve. To analyze the unknown samples, the circular dichroism spectra of the samples (amounts provided in section 2.3.10 to 2.3.14) were converted into enantiomeric excess values. The averages and standard deviations were calculated from the enantiomeric excess values of multiple replicate samples.

$$enantiomeric\ excess = \left[\frac{|x_l - x_d|}{x_l + x_d} \right] \textbf{x100} \qquad \text{(Equation 2)}$$

2.3.7. Preparation of racemic powder

Racemic mixtures were prepared by mixing equal amounts of enantiomorphic crystals from either homochiral single crystals or powder generated from the Kondepudi melt crystallization method. These mixtures were analyzed using circular dichroism to confirm a 50:50 mixture.

2.3.8. Viedma deracemization-stirring mechanism

A sample of racemic powder (0.25 g) and grinding media (3.0 g of 0.8 mm YTZ® Zirconia ceramic beads) were suspended in a pre-saturated solution of the same molecule (1 mL, specified solvent) in a sealed round bottom flask (5 mL). The sample was then stirred with a stir bar (oval shape, 10 mm x 4 mm) at 2400 rpm unless otherwise specified. Slurry samples were collected at specified times using a Pasteur pipet (*ca.* 100 μL sample) and deposited on a filter paper to dry prior to circular dichroism analysis. The amount of solvent collected was replenished in the reaction vessel after each sampling.

2.3.9. Viedma deracemization-shaking mechanism

A sample of racemic powder (0.20 g) and grinding media (*ca.* 1.2 g of 1.4 mm ceramic beads) with pre-saturated solvent (400 μL, specified solvent) was suspended in an MP Lysing matrix D eppendorf tube (2 mL). The samples were then shaken at a speed of 5 m/s for 40 seconds. This process was repeated 10 to 20 times with 5 minute cooling intervals. The samples were then transferred to filter paper to dry prior to circular dichroism analysis. Once dried, the solid was collected by separating the beads and powder with a 0.5 mL centrifuge filter (*ca.* 0.5 mm pores) and shaking it for several seconds in an eppendorf tube (2 mL). To investigate the potential of the liquid assisted conditions during the Viedma deracemization process, different volumes of pre-saturate solution were added (400 μL, 200 μL, 100 μL, 50 μL, 25 μL and 5 μL).

2.3.10. Directed mirror-symmetry breaking

Chiral additives, (R)-methylbenzylamine, (S)-methylbenzylamine, [(R), (S)]-*cis*-1-amino-2-indanol and [(S), (R)]-cis-1-amino-2-indanol were added in small amounts (specified in section 2.3.12) and the Viedma deracemization process was carried out as described above (section 2.3.9).

2.3.11. Benzil

Crystallization of benzil was carried out by dissolving *ca.* 10.1 g in xylenes (100 mL). Crystals were obtained after approximately 10 to 14 days of crystallization. When performing melt stirred crystallization, *ca.* 2 g of benzil was used. The melt powders were analyzed by circular dichroism and racemic mixtures were prepared from the appropriate mixture of left- and right-handed powders. Solubility measurements were carried out using acetone. For analysis, by Nujol, 6 mg of benzil was weighed using a microbalance and mixed with 67 mg of Nujol until homogenous. For KBr pellets, 3 mg of benzil was weighed using a microbalance and mixed together with 500 mg of dry KBr with a mortar and pestle until a thoroughly mixed fine powder was obtained. Circular dichroism spectra were scanned from 450 to 300 nm. A Nujol calibration curve was used for the stirring Viedma deracemization and a KBr calibration curve was used for the shaking Viedma deracemization. When generating the Nujol calibration curve, three samples were prepared and analyzed. The calibration curve was constructed from (±) 100%, (±) 50% and 0% enantiomeric excess mixtures. The average of the (±) 100% and 0% enantiomeric excess spectra of benzil are shown in Figure 14 A. Additional Nujol mull were prepared and scanned when the data was less reproducible. When generating the calibration curve by KBr, three samples were prepared and from each of these three samples, one KBr pellets was made. The calibration curve was constructed from (±) 100%, and 0% enantiomeric excess mixtures. Additional KBr pellets were prepared and scanned when the data was less reproducible. In preparation for the Viedma deracemization, acetone was used as the solvent for the saturated solution. For the analysis of the Viedma deracemization by stirring, three Nujol mull samples were prepared. These mull were analyzed and the enantiomeric excess was determined using the calibration curve. Additional mulls were scanned when the data showed high variability. For the analysis of the Viedma deracemization by shaking, three KBr pellets

were prepared. These pellets were analyzed and the enantiomeric excess was determined using the calibration curve. Additional samples were scanned when the data showed high variability. When performing the directed chiral amplification, 30 and 15 µL of methylbenzylamine were added and *ca.* 25 mg of *cis*-1-amino-2-indanol was added.

2.3.12. Diphenyl Disulfide

Crystallization of diphenyl disulfide was carried out by dissolving *ca.* 20 g in acetone (120 mL). Crystals were obtained after approximately 3 to 5 days. When performing melt stirred crystallization, *ca.* 2 g of diphenyl disulfide was used. The melt powders were analyzed by circular dichroism and racemic mixtures were prepared from the appropriate mixture of left- and right-handed powders. Solubility measurements were carried out using acetone. For analysis, 6 mg of diphenyl disulfide was weighed using a microbalance and mixed together with 500 mg of dry KBr with a mortar and pestle until a thoroughly mixed fine powder was obtained. Circular dichroism spectra were scanned from 400 to 250 nm. When generating the calibration curve, two samples were prepared and from each of these two samples, three KBr pellets were made. From each pellet, two different areas were scanned for a total of 12 circular dichroism curves. The calibration curve was constructed from (±) 100%, (±) 75%, (±) 50%, (±) 25% and 0% enantiomeric excess mixtures. The average of the (±) 100% and 0% enantiomeric excess spectra of diphenyl disulfide are shown in Figure 15 A. Additional KBr pellets were prepared and scanned when the data was less reproducible. In preparation of the Viedma deracemization, acetone was used as the saturated solution. For the Viedma deracemization, due to the small amount of sample collected at each time, only one sample per KBr mixture was made. Two pellets were generated from this mixture and two different areas (for a total of four) were analyzed by circular dichroism circular dichroism and converted to enantiomeric excess. Additional KBr pellets were made and scanned when the data showed high variability.

2.3.13. Benzophenone

Crystallization of benzophenone was carried out by dissolving *ca.* 40.0 g in acetone (70 mL). Crystals were obtained after approximately 3 to 5 days. When performing melt stirred crystallization, *ca.* 3 g of benzophenone was used and the melt was seeded with either left- or right-handed single crystals 1 °C below the melting point, while it is still a melt. The melt powders were analyzed by circular dichroism and racemic mixtures were prepared from the appropriate mixture of left- and right-handed powders. Solubility measurements were carried out using acetone. For analysis, 4 mg of benzophenone was weighed using a microbalance and mixed together with 500 mg of dry KBr using a mortar and pestle until a thoroughly mixed fine powder was obtained. Circular dichroism spectra were scanned from 400 to 250 nm. When generating the calibration curve, three samples were prepared, and from each of these samples, two KBr pellets were made. Each pellet was analyzed for a total of 6 curves. The calibration curve was constructed from (±) 100%, (±) 50% and 0% enantiomeric excess mixtures. The average of the (±) 100% and 0% enantiomeric excess spectra of benzophenone are shown in Figure 16 A. Additional KBr pellets were prepared and scanned when the data was less reproducible. In preparation of the Viedma deracemization, acetone was used as the saturated solution. During the Viedma deracemization experiments, the stirring speed was set at 3600 rpm instead of 2400 rpm since the crystals were too large to sample at 2400 rpm. For the analysis of the Viedma deracemization of benzophenone, one KBr pellet was prepared from three separate samples. These pellets were analyzed and the enantiomeric excess was determined using the calibration curve. Additional samples were scanned when the data showed high variability.

2.3.14. Butylated hydroxytoluene

Crystallization of butylated hydroxytoluene was carried out by dissolving *ca.* 28.0 g in 95% ethanol (200 mL). Crystals were obtained after approximately 2 to 3 days. When performing melt stirred crystallization, *ca.* 3 g of butylated hydroxytoluene was used and the melt was seeded with either left- or right-handed single crystals 1 °C below the melting point, while it is still a melt. The melt powders were analyzed by circular dichroism and racemic mixtures were prepared from the appropriate mixture of left-handed and right-handed powders. Solubility measurements were carried out using acetone. For analysis, 10 mg of butylated hydroxytoluene was weighed using a microbalance and mixed together with 500 mg of dry KBr with a mortar and pestle until a thoroughly mixed fine powder was obtained. Circular dichroism spectra were scanned from 350 to 250 nm. When generating the calibration curve, three samples were prepared, and from each of these samples, two KBr pellets were made. Each pellet was analyzed for a total of 6 curves. The calibration curve was constructed from (±) 100%, (±) 50% and 0% enantiomeric excess mixtures. The average of the (±) 100% and 0% enantiomeric excess spectra of butylated hydroxytoluene are shown in Figure 17 A. Additional KBr pellets were prepared and scanned when the data was less reproducible. In preparation of the Viedma deracemization, acetone was used as the saturated solution. For the analysis of the Viedma deracemization of butylated hydroxytoluene, six KBr pellets prepared from three separate samples (2 pellets per samples). These pellets were analyzed and the enantiomeric excess was determined using the calibration curve. Additional samples were scanned when the data showed high variability.

2.3.15. Tetraphenylethylene

Crystallization of tetraphenylethylene was carried out by dissolving *ca.* 3 g in toluene (110 mL). Crystals were obtained after approximately 5 to 7 days. The racemic powder was

taken from the bottle since circular dichroism spectrum displayed a 0% enantiomeric excess. Solubility measurements were carried out using a toluene. For analysis, 3 mg of tetraphenylethylene was weighed using a microbalance and mixed together with 500 mg of dry KBr with a mortar and pestle until a thoroughly mixed fine powder was obtained. Circular dichroism spectra were scanned from 400 to 250 nm. For generating the calibration curve, three samples were prepared, and from each of these samples, one KBr pellet was made. Each pellet was analyzed for a total of 3 curves. The calibration curve was constructed from (±) 100%, (±) 50% and 0% enantiomeric excess mixtures. The average of the (±) 100% and 0% enantiomeric excess spectra of tetraphenylethylene are shown in Figure 18 A. Additional KBr pellets were prepared and scanned when the data was less reproducible. In preparation for Viedma deracemization, toluene was used as the solvent for the saturated solution. For the analysis of the Viedma deracemization of tetraphenylethylene, one KBr pellet was prepared from three separate samples. These pellets were analyzed and the enantiomeric excess was determined using the calibration curve. Additional samples were scanned when the data showed high variability.

3. Results and discussion

3.1. Generality of the Viedma deracemization process

In general, approaches of analyzing chirality in solid samples consist of using optical methods such as polarized light microscopy, polarimetry and circular dichroism.[40] In this project, the method most often used to analyze chiral crystals was solid-state circular dichroism, the differential absorption of circularly polarized light. Solid-state circular dichroism has been used frequently for qualitative analysis of chiral molecules. Some examples include the investigation of natural products,[105] chiral metal-organic frameworks, [106-108] organic films,[109,110] chiral metal complexes[111-113] as well as synthetic chiral organic compounds.[114,115] The major focus of this work is the investigation of crystal chirality from achiral compounds. Since chirality is only observed in the crystalline state for achiral molecules, only solid-state optical methods can be conducted to analyze the chirality. Solid-state circular dichroism can also be used to investigate the chirality of achiral molecules that self-assemble into chiral structures such as the investigation of chiral metal-organic frameworks starting from achiral molecules,[116,117] organic compounds,[99,118-121] and metal complexes.[122,123] In this work, the importance of using solid- state circular dichroism, as both a qualitative and quantitative methods, to characterize the chirality and determine the enantiomeric excess was demonstrated for five achiral conglomerate systems that underwent the Viedma deracemization process.

3.1.1. Chiral crystallization

Chiral crystallization was carried out to: (*i*) determine the crystal chirality distribution, (*ii*) obtain single enantiopure crystals for calibration curves and (*iii*) make racemic mixtures for Viedma deracemization.

Benzil

Chiral crystallization of benzil (crystallized from xylenes) generated a distribution ratio of 56:49 of M- to P-form crystals. Characterization of benzil crystals was carried out using polarized light microscopy, polarimetry and circular dichroism (Figure 14 A). Benzil was the only system where polarized light microscopy was used to analyze the optical rotatory dispersion of the left- and right-handed crystals, since the optical face is easily found and relatively prominent (Figure 14 B). Using polarized light microscopy, M-form single crystals exhibited an optical dispersion from amber to clear to blue and P-form single crystals exhibited an optical dispersion from amber to blue to clear. SHAPE was used to index and visualize the morphology of the crystals and the [001] face, the optical face, is highlighted in Figure 14 C. When performing polarimetry, an optical rotation of ± 28.4°/mm was obtained, which is in close agreement with the literature value of ± 24.8°/mm.[25] By solid-state circular dichroism, the M-form single crystal exhibited positive peaks with maxima at approximately 400 and 340 nm and the P-form single crystals exhibited a mirror image spectrum. The obtained spectra were in agreement with the literature.[118] Absorptions at 400 and 340 nm correspond to visible and near UV energy n→π* transitions, respectively.[118] A circular dichroism signal of *ca.* 0 was observed when mixing a 1:1 weight ratio of M- to P-form crystals (Figure 16 A).

Figure 14. (A) Solid-state circular dichroism spectra of benzil (Nujol) (B) benzil crystal from xylenes (C) major faces of a benzil crystal visualized with SHAPE V7.2

Diphenyl disulfide

Chiral crystallization of diphenyl disulfide (crystallized from acetone) generated a distribution ratio of 34:18 of M- to P-form crystals. By solid-state circular dichroism, the M-form single crystal exhibited two positive peaks with maxima at approximately 313 and 260 nm and the P-form single crystals exhibited a mirror image spectrum (Figure 15 A). The obtained spectra were in agreement with the literature.[120] Absorptions at 313 and 260 nm correspond to two low energy n→σ* transitions.[124] A circular dichroism signal of *ca.* 0 was observed when mixing a 1:1 weight ratio of M- to P-form crystals (Figure 15 A).
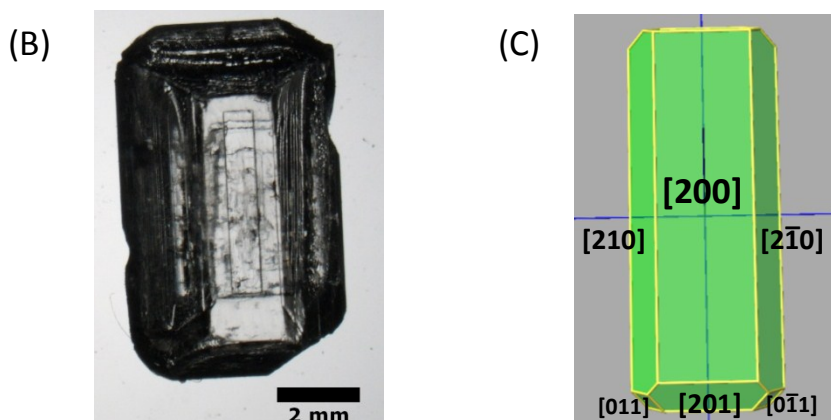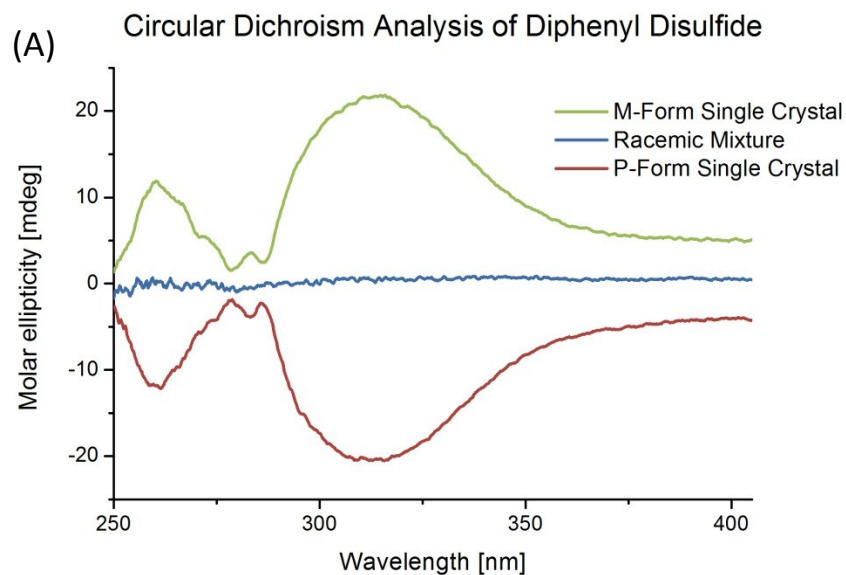
Figure 15. (A) Solid-state circular dichroism spectra of diphenyl disulfide (KBr) (B) diphenyl disulfide crystal from acetone (C) major faces of a diphenyl disulfide crystal visualized with SHAPE V7.2

Benzophenone

Chiral crystallization of benzophenone (crystallized from acetone) generated a distribution ratio of 17:8 of M- to P-form crystals. By solid-state circular dichroism, M-form single crystals exhibited three negative peaks and one positive peak with maxima at approximately 374, 359, 345 and 310 nm, respectively. The P-form single crystals exhibited a mirror image spectrum (Figure 16 A). The observed spectra were in agreement with the literature.[99] The peak ranging between 375 to 330 nm corresponds to a n→π* transition.[98] A

circular dichroism signal of *ca.* 0 was observed when mixing a 1:1 weight ratio of M- to P-form crystals (Figure 16 A).

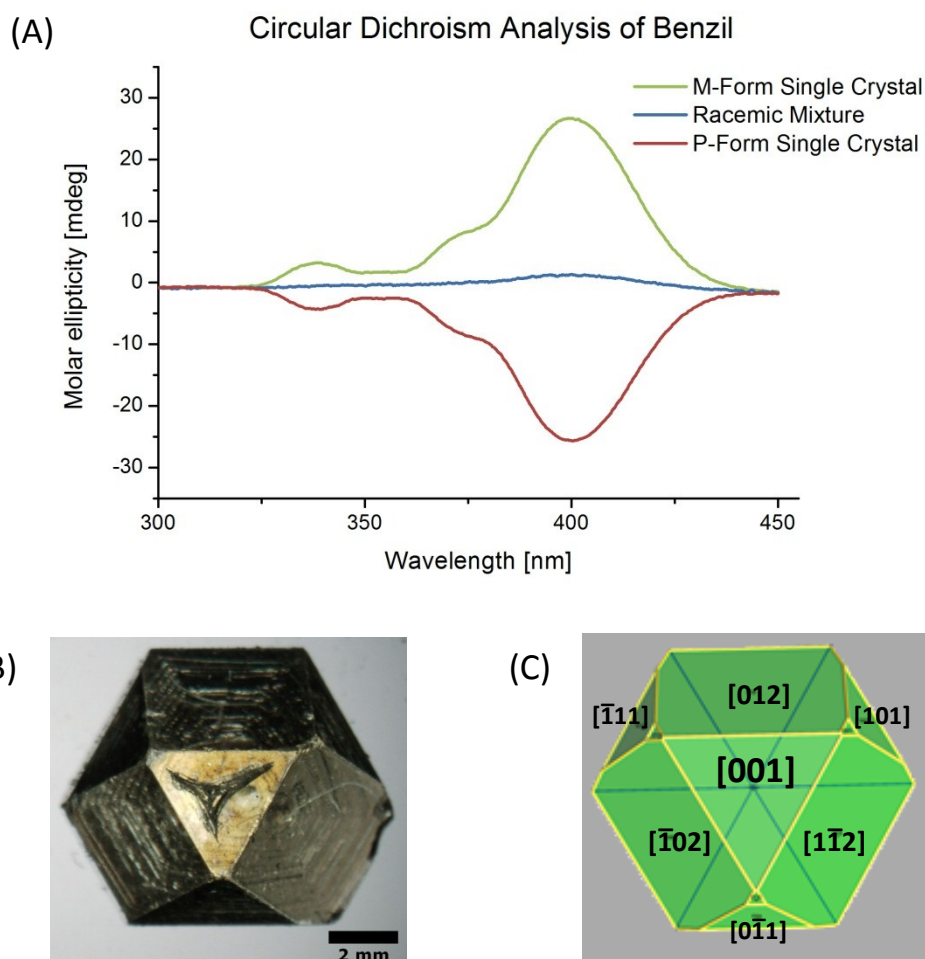**Figure 16.** (A) Solid-state circular dichroism spectra of benzophenone (KBr) (B) benzophenone crystal from acetone (C) major faces of a benzophenone crystal visualized with SHAPE V7.2

Butylated hydroxytoluene

Chiral crystallization of butylated hydroxytoluene (crystallized from ethanol) generated a distribution ratio of 39:5 of left-handed ([+] circular dichroism signal) to right handed ([-] circular dichroism signal) crystals. By solid-state circular dichroism, the left-handed crystals exhibited a positive peak with a maximum at approximately 287 nm and the right-handed crystals exhibited a mirror image spectrum (Figure 17). The obtained spectra were in agreement

with the literature.[125]   A circular dichroism signal of *ca.* 0 was observed when mixing a 1:1 weight ratio of left to right handed crystals (Figure 17 A).

(A) Circular Dichroism Analysis of Butylated Hydroxytoluene

(B)

(C)
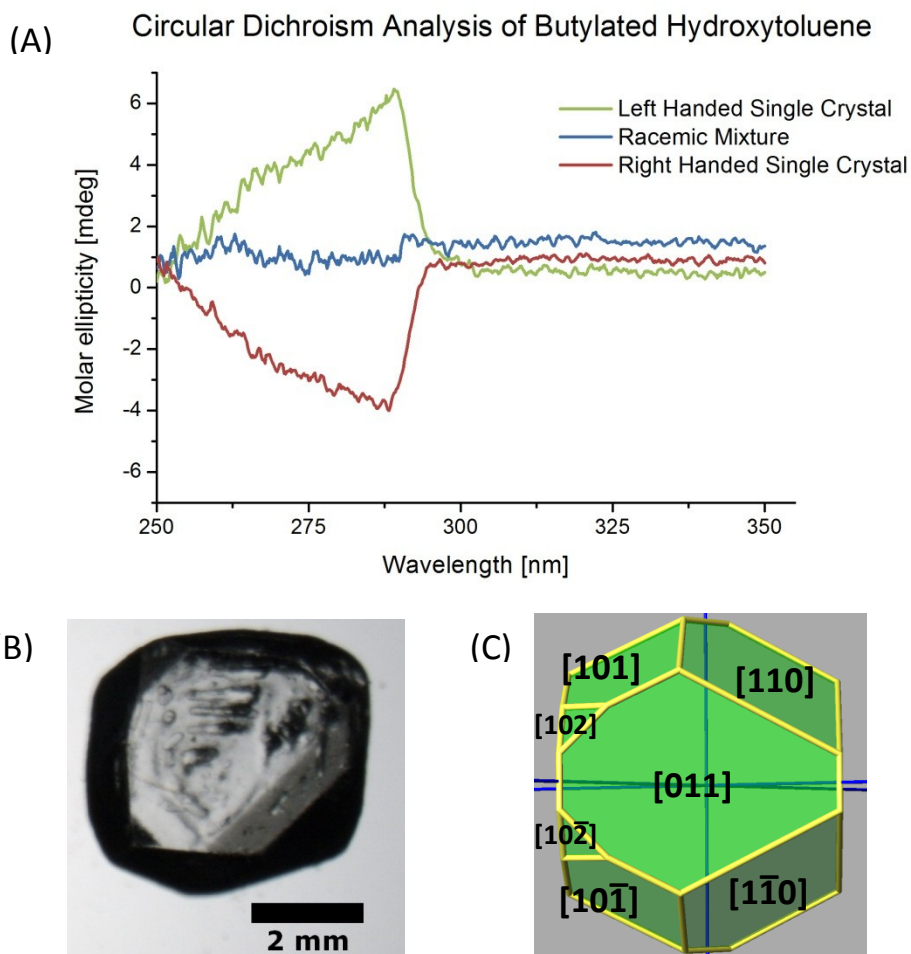
Figure 17. (A) Solid-state circular dichroism spectra of butylated hydroxytoluene (KBr) (B) butylated hydroxytoluene crystal from ethanol (C) major faces of a butylated hydroxytoluene crystal visualized with SHAPE V7.2

Tetraphenylethylene

Chiral crystallization of tetraphenylethylene (crystallized from toluene) generated a distribution ratio of 14:26 of left-handed ([+] circular dichroism signal at 360 nm) to right handed ([-] circular dichroism signal at 360 nm) crystals. By solid-state circular dichroism, left-handed crystals exhibited two positive peaks and one negative peak with maxima at approximately 360, 280 and 260 nm, respectively. The right-handed crystals exhibited a mirror image spectrum (Figure 18 A). The obtained spectra were in agreement with the literature.[119]

The peak at 260 nm corresponds to a π→π*transition.[126] A circular dichroism signal of *ca.* 0 was observed when mixing a 1:1 weight ratio of left- to right-handed crystals (Figure 18 A).
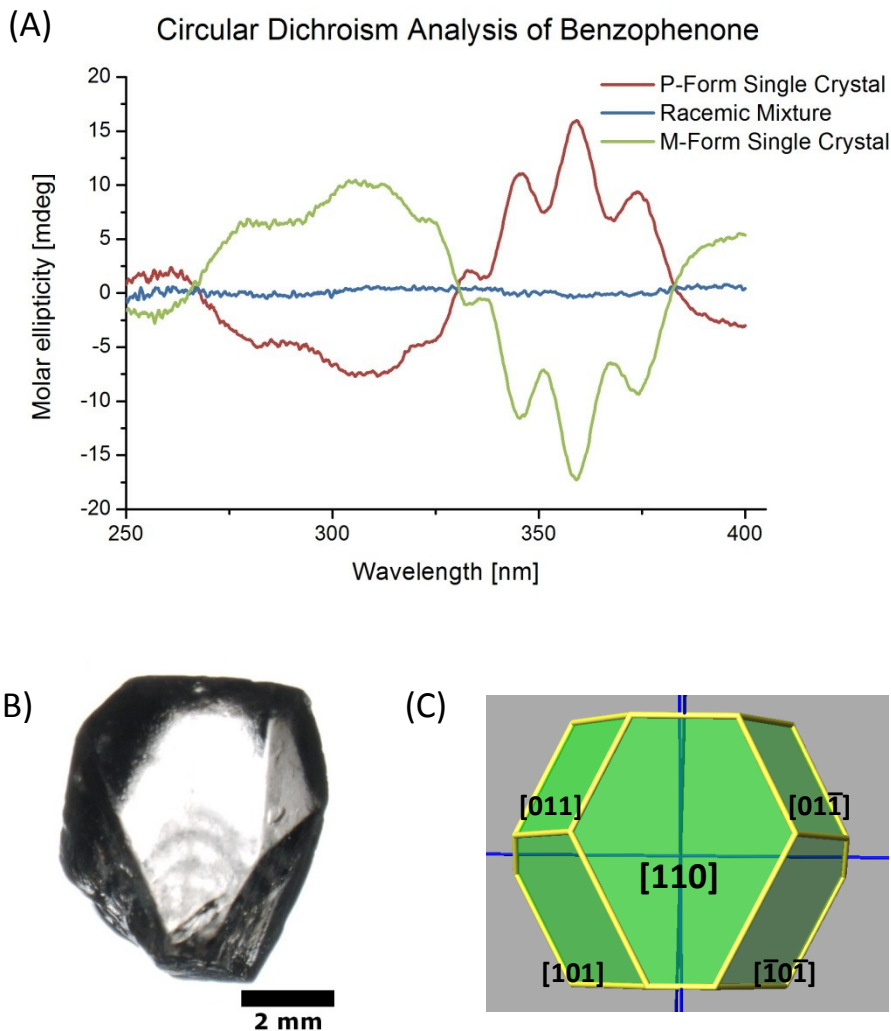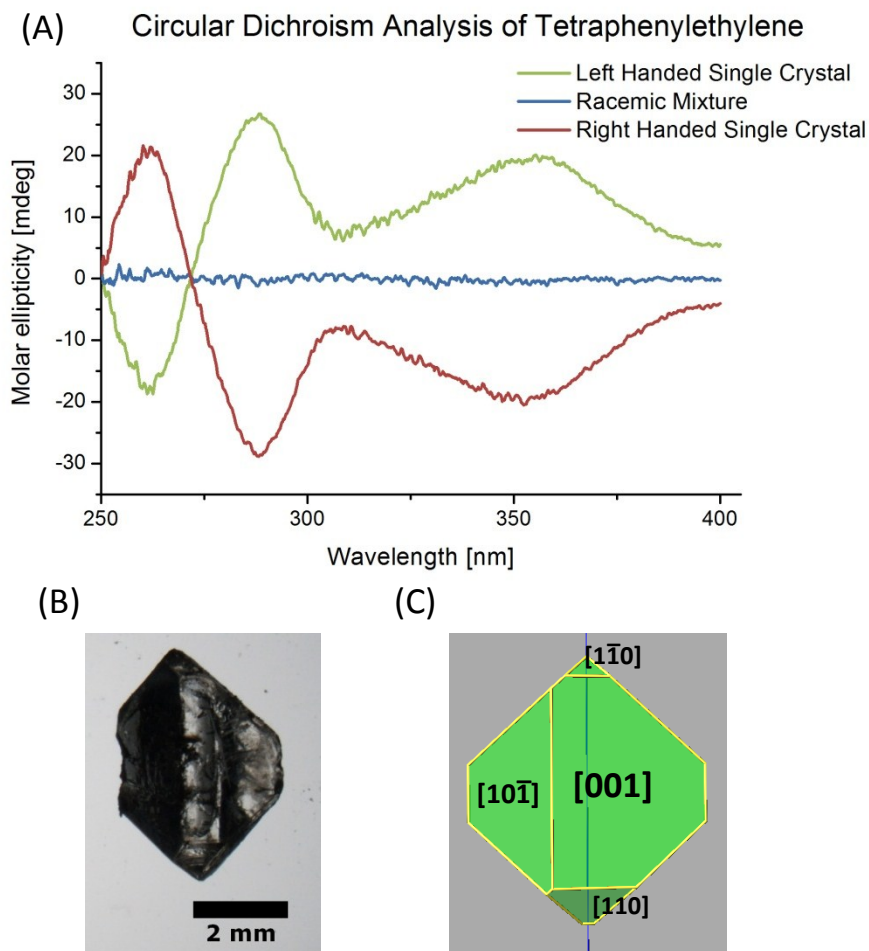

Figure 18. (A) Solid-state circular dichroism spectra of tetraphenylethylene (KBr) (B) tetraphenylethylene crystal from toluene (C) major faces of a tetraphenylethylene crystal visualized with SHAPE V7.2

Different ratios of left- to right-handed chiral crystals were obtained for each system. With the exception of benzil, non-stochastic chiral crystallization was observed for all system. Without a chiral influence, there is an expected 50% chance of generating left-handed or right-handed crystals (*i.e.* a stochastic distribution).

A binomial statistical test was conducted to evaluate whether the obtained results agree within the limits for generating a stochastic ratio of left- to right-handed crystals (the null

hypothesis) based on the number of counted crystals. The binomial test allows one to determine whether the results obtained are statistically significant compared to the null hypothesis.[127] A binomial test can only be conducted if: (*i*) the system has a set number of events (N), (*ii*) during each event, the observations are independent of one another, (*iii*) the system only has two outcomes and (*iv*) the probability between each outcome does not change over time.[127] In this investigation, a set number of left- and right-handed single crystals were counted and assumed to have crystallized without any external influences and with a 50% chance of generating either a left- or right-handed crystal. A binomial probability, the probability that the results obtained were random, was calculated for each system (Table 4). In general, a probability below 0.05 (5%) signifies that the system did not follow the null hypothesis and a bias is likely present. Since diphenyl disulfide, benzophenone, butylated hydroxytoluene and tetraphenylethylene had binomial probabilities below 5%, it signifies that a bias likely affected the crystallization ratios obtained. For benzil, under a set number of events, the binomial probability is above the standard 5% cut-off value, indicating that the crystallization ratio deviation from 50% is not statistically significant at the 95% confidence level.

Table 4. Results of the binomial test for chiral crystallization based on a 50% chance probability

Molecular system	Number of Events (N)	Left-handed (M-form) crystals	Right-handed (P-form) crystals	Binomial probability
Benzil	105	56	49	6.16×10^{-2}
Diphenyl disulfide	52	34	18	9.48×10^{-3}
Benzopheone	25	17	8	3.22×10^{-2}
Butylated hydroxytoluene	44	39	5	6.16×10^{-8}
Tetraphenylethylene	40	14	26	2.11×10^{-2}

The biased crystallization ratio for diphenyl disulfide, benzophenone, butylated hydroxytoluen and tetraphenylethylene could be explained with cryptochiral seeding. As explained by Pincock *et al.*,[90] the world is filled with chirality, it is relatively easy to rationalize

the contamination of a solution with chiral dust or skin particles. The cryptochiral seeds could preferentially drive these crystals to grow to a certain enantiomorph. Examples of preferential crystallization, possibly due to a cryptochiral environment, have also been reported in the literature. These include the crystallization of helical triallylamine copper chloride (only M-form crystals were obtained during crystallization),[92] crystallization of diphenyl ditelluride (out of 10 crystals, all showed the same handedness)[120] and in the crystallization of sodium chlorate (a series of crystallization generated a significantly higher number of left- compared to right-handed crystals).[59] An attempt to 'generate' a cryptochiral environment using amino acids with concentrations ranging in the parts per billion (ppb) was carried out by Veintemillas-Verdaguer *et al*.[128] They demonstrated that a phenylalanine concentration of 2 ppb generated a ratio of 2:1 of left- to right-handed sodium chlorate crystals. Another factor that can influence the distribution ratio is the fragmentation of crystal clusters during crystallization. The fragments would seed the solution and drive the crystals in the dish to have one handedness (*e.g.* in the crystallization of diphenyl disulfide and butylated hydroxytoluene the majority crystallization dishes had crystals with one handedness). It is also possible that the sample size distribution is too small, skewing the obtained results towards a preferred handedness.

These results demonstrate the sensitivity of chiral crystallization towards a cryptochiral environment thus preventing non-stochastic crystallization. For example, it is surprising that only 10% of *ca.* 50 crystals of butylated hydroxytoluene were right handed when a 50:50 mixture is expected. However, a similar result was observed in the crystallization of sodium chlorate.[59] Out of 240 crystals, Viedma observed that only 4 were right-handed, making this phenomenon less unusual. It is important to realize that a cryptochiral environment could also affect the Viedma deracemization process by breaking the mirror symmetry and directing the asymmetric amplification. This was observed previously in our lab in the Viedma

deracemization of ethylenediammonium sulfate, where 95% of experiments amplified towards levorotatory crystals.[61] Finally, as stated by Viedma, a cryptochiral environment from an unknown source could have also played a role in breaking the mirror symmetry during the chiral amplification of biological molecules.[59]

3.1.2. Enantiomeric excess curves

Solid-state circular dichroism is a very powerful tool to determine enantiomeric excess quantitatively.[129] One of the first examples of using solid-state quantitative analysis was reported in 2005.[130] Hakansson *et al.* generated a calibration curve of 7 different coordinate lanthanide systems that form interconverting chiral propellers to determine the enantiomeric excess of the bulk system.[130] Some other examples include: (*i*) the enantiomeric excess quantification changes of metal-frameworks made from achiral precursors[117] and determining the bulk enantiomeric excess of chiral metal complexes.[130-133] The complexes investigated were the achiral aluminum tris(2,6-diphenylphenoxide),[131] chiral copper(I)[132] and copper(II) halides [132] as well as chiral zinc(II) chloride.[132] In our research, quantitative solid-state circular dichroism was used to monitor the enantiomeric excess of samples undergoing Viedma deracemization with time.

There are two main methods for analyzing samples by solid-state circular dichroism: (*i*) the KBr method and (*ii*) the Nujol mull method. Both methods have advantages and limitations. The main limitations for both methods are absorption flattening, light scattering, turbidity and inhomogeneity of the sample.[126,134-136] Often times when obtaining a circular dichroism spectrum, a change in absorption and shifts in absorption peaks are observed. These and other artefacts of the spectrum are believed to be caused by light scattering and reflections of the sample due to the variable size distribution of the crystals.[135] Some of these issues can be minimized by optimizing the sample preparation and concentration, repeating the experiment

and placing the sample close to the detector to limit light scattering.[134] Each system underwent a concentration optimization by finding the right weight to obtain maximal molar ellipticity signal with a low voltage.

The advantage of the Nujol mulls is that sample preparation is relatively quick and they generate low voltage since the sample can often be relatively transparent and homogeneous. However, Nujol mull spectra are quite difficult to reproduce and sometimes did not generate a circular dichroism spectrum (*i.e.* diphenyl disulfide and butylated hydroxytoluene). For example, it was sometimes difficult to grind a solid/Nujol mixture to yield a homogeneous sample with a uniform crystal size distribution and a reproducible sample thickness between the quartz windows.[135]

On the other hand, the KBr sample preparation method works well for most systems and it provides more reproducible spectra. When clear pellets were obtained, they behave like a lens which 'naturally' focuses scattered light towards the detector by the *Shibata opal glass method* (*i.e.* using an additional lens to focus scattered light into the detector).[134] In addition, the crystal size distribution will be similar to the KBr matrix since the powder mixture is ground together.[135] However, KBr is hygroscopic and quickly becomes opaque when exposed to air, which results in more light scattering.[134] Sample inhomogeneity in KBr pellets can also be an issue, as it is hard to get a homogeneous mixture of solids. This can cause signal variation due to different concentrations throughout the pellet.

Benzil

A calibration curve was generated by taking different weight ratios of left- and right-handed crystals at a constant mass as described in section 2.3.11. The weighed crystals were mixed with Nujol, placed between two circular quartz plates and scanned by circular dichroism

where the peak at 400 nm was utilized for the calibration curve (Figure 19). An R^2 value of 0.999 was obtained.

Figure 19. Calibration curve of Benzil at 400 nm using Nujol

A calibration curve was also generated by taking different weight ratios of left- and right-handed crystals at a constant mass as described in section 2.3.11. The weighed crystals were mixed with KBr, made into a pellet and scanned by circular dichroism where the peak at 399 nm was utilized for the calibration curve (Figure 20). An R^2 value of 0.999 was obtained.
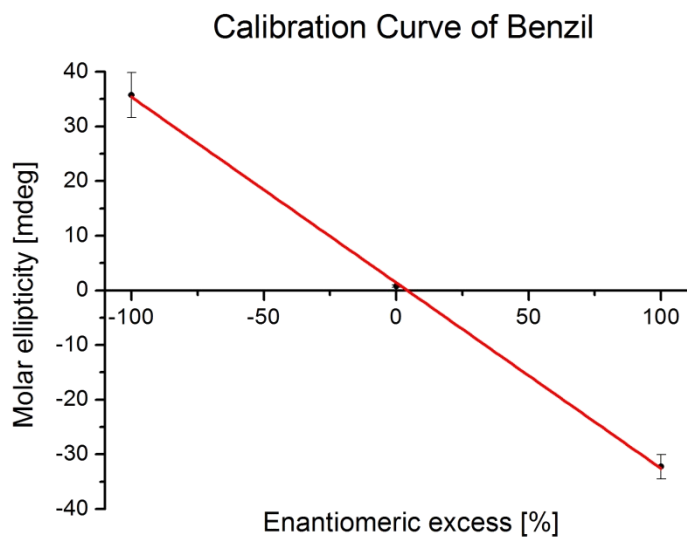
Figure 20. Calibration curve of Benzil at 399 nm using KBr

Diphenyl Disulfide

A calibration curve was generated by taking different weight ratios of left- and right-handed crystals at a constant mass as described in section 2.3.12. The weighed crystals were mixed with KBr, made into a pellet and scanned by circular dichroism where the peak at 313 nm was utilized for the calibration curve (Figure 21). An R^2 value of 0.989 was obtained.
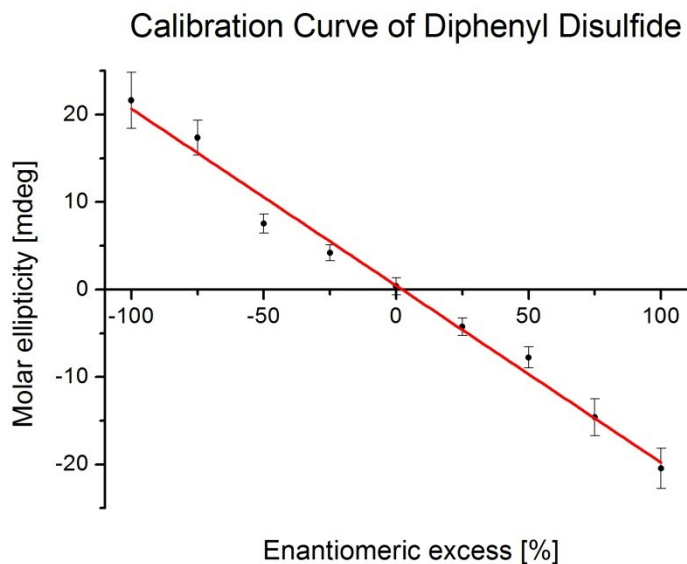
Figure 21. Calibration curve of diphenly disulfide at 313 nm using KBr

Benzophenone

A calibration curve was generated by taking different weight ratios of left- and right-handed crystals at a constant mass as described in section 2.3.13. The weighed crystals were mixed with KBr, made into a pellet and scanned by circular dichroism where the peak at 359 nm was utilized for the calibration curve (Figure 22). An R^2 value of 0.995 was obtained.
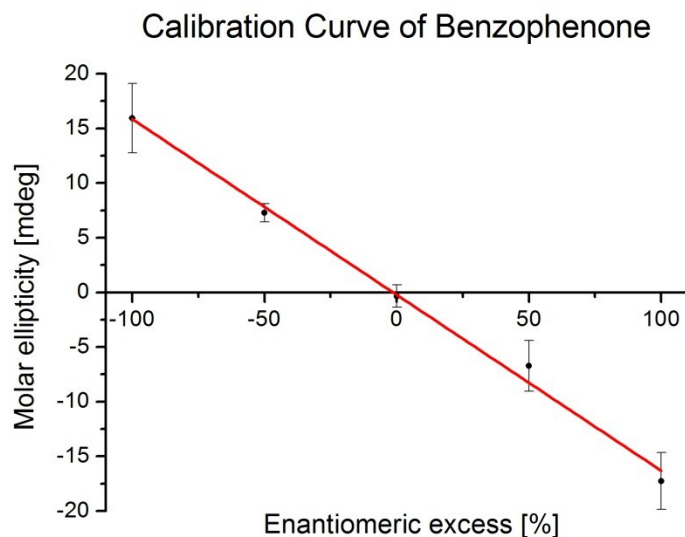
Figure 22. Calibration curve of benzophenone at 359 nm using KBr

Butylated Hydroxytoluene

A calibration curve was generated by taking different weight ratios of left- and right-handed crystals at a constant mass as described in section 2.3.14. The weighed crystals were mixed with KBr, made into a pellet and scanned by circular dichroism where the peak at 285 nm was utilized for the calibration curve (Figure 23). An R^2 value of 0.957 was obtained.
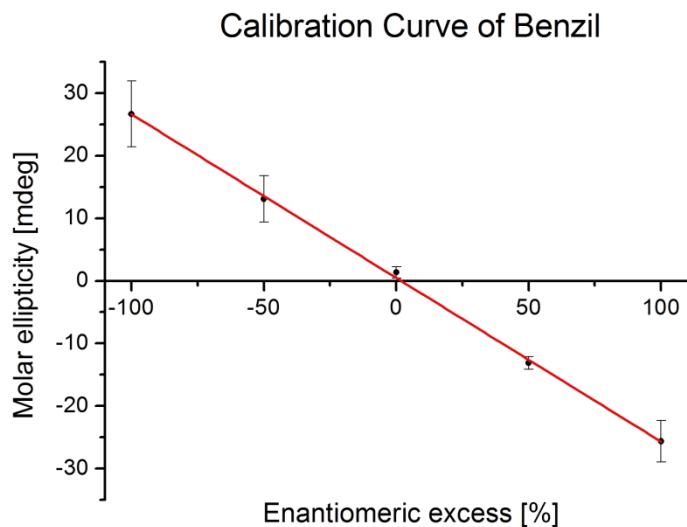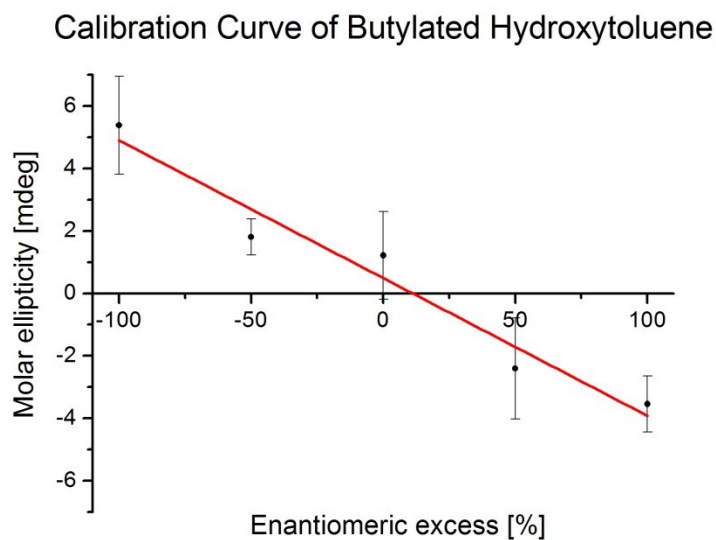

Figure 23. Calibration curve of butylated hydroxytoluene at 285 nm using KBr

Tetraphenylethylene

A calibration curve was generated by taking different weight ratios of left- and right-handed crystals at a constant mass as described in section 2.3.15. The weighed crystals were mixed with KBr, made into a pellet and scanned by circular dichroism where the peak at 355 nm was utilized for the calibration curve (Figure 24). An R^2 value of 0.997 was obtained.
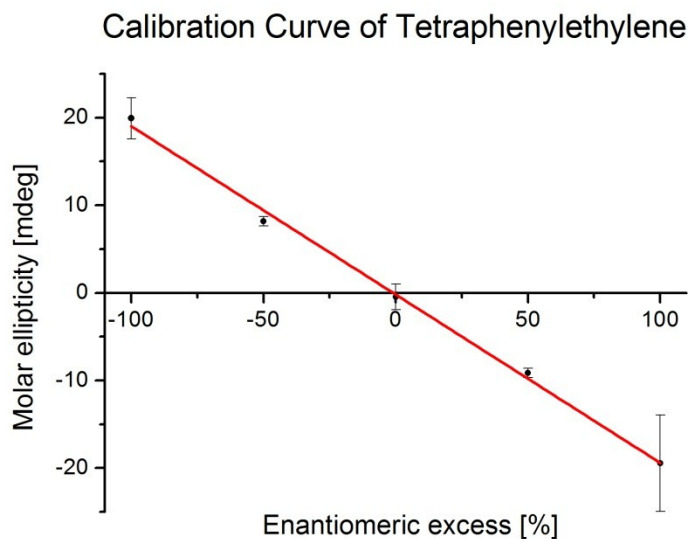

Figure 24. Calibration curve of tetraphenylethylene at 355 nm using KBr

For all systems, higher signal variation (*ca.* ± 5 mdeg for KBr and *ca.* ± 10 mdeg for Nujol) was observed at higher percent enantiomeric excess values. Correspondingly, at lower enantiomeric excess values, smaller signal variations were observed (*ca.* ± 3 mdeg for both KBr and Nujol). KBr pellets appear to give more reproducible pellets then those carried out by Nujol mull (high standard deviation). This could be due to the larger crystal size distribution obtained in the Nujol mull.[135] Apart from benzil, the results obtained using Nujol generated either low signal-to-noise ratios (tetraphenylethylene and benzophenone) or no signal at all (butylated hydroxytoluene and diphenyl disulfide).

The R^2 values for all calibration curves were roughly 0.98 except for butylated hydroxytoluene at 0.96 (Figure 23). This exception for butylated hydroxytoluene is expected

since the maximum circular dichroism absorption for homochiral butylated hydroxytoluene is only *ca.* 4 mdeg (*i.e.* a very low signal-to-noise ratio).

3.1.3. Asymmetric amplification

Homochirality for five different achiral conglomerate systems was reached with 2 to 30 hours under the Viedma deracemization process. Analysis was carried out using the generated calibration curves discussed in section 3.1.2 (Figures 19, 21-24).

Benzil

Asymmetric amplification of benzil under attrition-enhanced conditions took approximately 2.5 hours when starting with a nearly racemic mixture (Figure 25). The amplification of benzil was attempted 9 times, and an amplification ratio of 1:8 M- to P-form was observed.

Figure 25. Viedma deracemization of benzil starting with 0.25 g of a racemic mixture, 3.00 g of 0.8 mm ceramic beads, 1 mL of pre-saturated acetone and stirred at 2400 rpm

Diphenyl disulfide

Asymmetric amplification of diphenyl disulfide under attrition-enhanced conditions took approximately 8 hours when starting with a nearly racemic mixture (Figure 26). The

amplification of diphenyl disulfide was attempted 9 times, and an asymmetric amplification ratio of 3:6 M- to P-form was observed.

Figure 26. Viedma deracemization of diphenyl disulfide starting with 0.25 g of a racemic mixture, 3.00 g of 0.8 mm ceramic beads, 1 mL of pre-saturated acetone and stirred at 2400 rpm

Benzophenone

Asymmetric amplification of benzophenone under attrition-enhanced conditions took approximately 24 hours when starting with a nearly racemic mixture (Figure 27). The amplification of benzophenone was attempted 2 times, and an asymmetric amplification ratio of 2:0 M- to P-form was observed.

Figure 27. Viedma deracemization of benzophenone starting with 0.25 g of a racemic mixture, 3.00 g of 0.8 mm ceramic beads, 1 mL of pre-saturated toluene and stirred at 3600 rpm

Butylated hydroxytoluene

Asymmetric amplification of butylated hydroxytoluene under attrition-enhanced conditions took approximately 26 hours when starting with a 20% enantiomeric excess (Figure 28). Mixing an equal amount of both enantiomorphic crystals to generate a racemic mixture was sometimes difficult due to static charging of the powders during grinding. The amplification of butylated hydroxytoluene was attempted 2 times, and an asymmetric amplification ratio of 1:1 left- to right-handed signals was observed.

Figure 28. Viedma deracemization of butylated hydroxytoluene starting with 0.25 g of a scalemic mixture, 3.00 g of 0.8 mm ceramic beads, 1 mL of pre-saturated acetone and stirred at 2400 rpm

Tetraphenylethylene

Asymmetric amplification of tetraphenylethylene under attrition-enhanced conditions took approximately 30 hours when starting with a nearly racemic mixture (Figure 29). The amplification of tetraphenylethylene was attempted 2 times, and an amplification ratio of 0:2 left- to right-handed crystals was obtained.
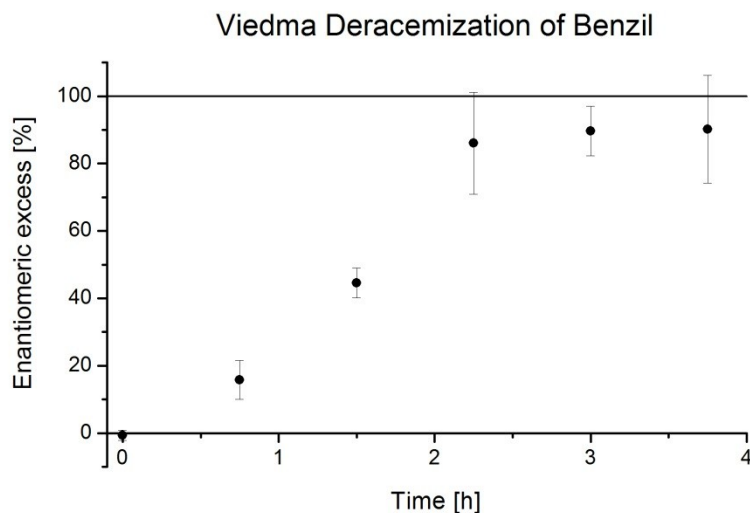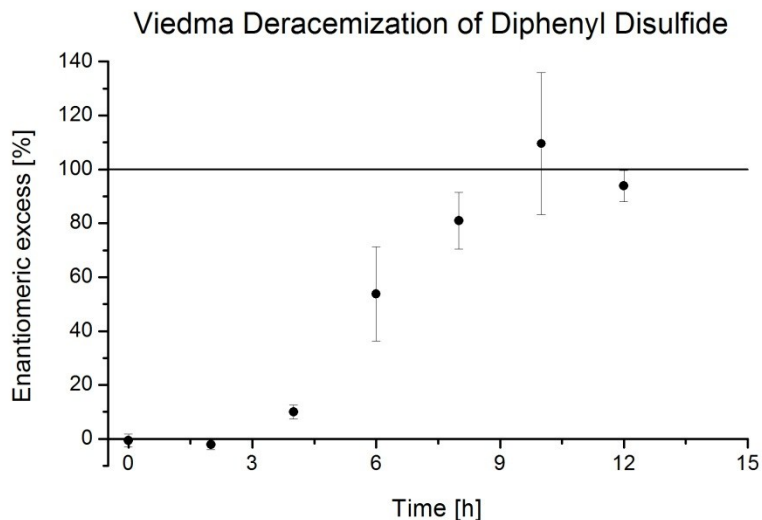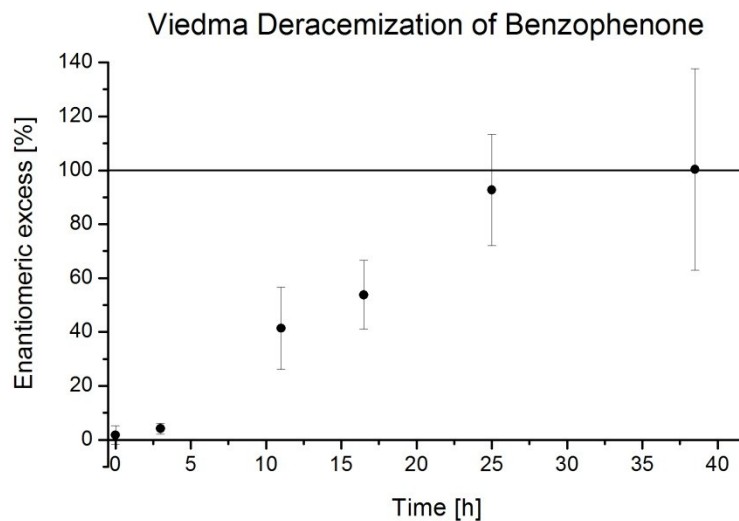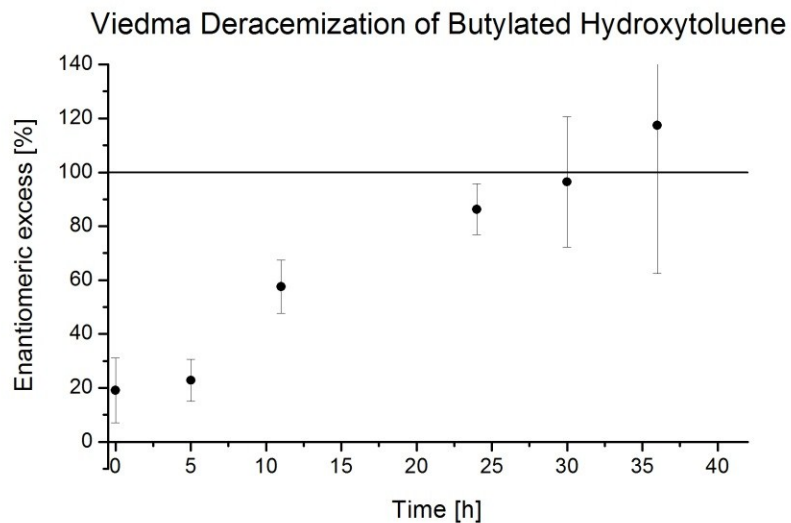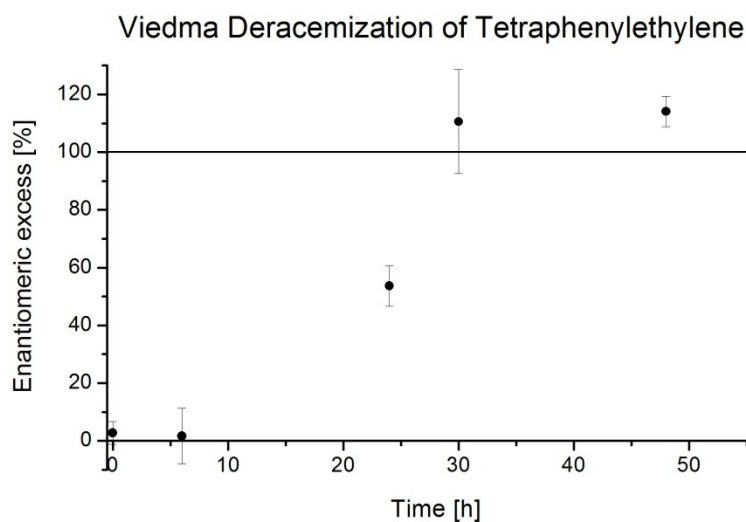

Figure 29. Viedma deracemization of tetraphenylethylene starting with 0.25 g of a racemic mixture, 3.00 g of 0.8 mm ceramic beads, 1 mL of pre-saturated toluene and stirred at 2400 rpm

Performing the Viedma deracemization process on these five systems, under attrition conditions, produced a solid-state transformation to homochirality as expected for conglomerate systems. In the literature, achiral molecules tend to amplify to homochirality within a few days, and these 5 systems agree with this time scale.[12,51,61] A summary of all the Viedma deracemization results are tabulated in Table 5.

Table 5. Tabulated data of each molecule that underwent the Viedma deracemization process (*N.B.* amp. means amplification)

Molecular system	Solvent	Grinding speed (rpm)	Solubility (g/mL)	Amp. time (h)	P-form amp.	M-form amp.
Benzil	acetone	2400	3.81×10^{-1}	2	1	8
Diphenyl disulfide	acetone	2400	2.27×10^{-1}	8	6	3
Benzopheone	acetone	3600	1.3×10^{0}	24	0	2
Butylated hydroxytoluene	acetone	2400	9.47×10^{-1}	26	1	1
Tetraphenylethylene	toluene	2400	1.78×10^{-2}	30	0	2

Different amplification times were observed for each molecular system under similar conditions (suspended in the same volume, same weight percent grinding media, and same grinding speed [except for benzophenone]). Note that the amplification rate is affected by three major factors: (*i*) racemization catalyst amount, (*ii*) attrition probability and (*iii*) probability of Ostwald ripening (solubility).[52] Since all the molecules investigated herein are achiral in solution, no racemization catalyst is required. Therefore, the key factors influencing Viedma deracemization for our systems are the attrition probability and the Ostwald ripening probability. Furthermore, as discussed in section 1.5, the efficacy of chiral cluster selective attachment must also be considered.

Noorduin *et al.* investigated the theoretical importance of attrition (to give smaller crystals) and Ostwald ripening (to give larger crystals) and found that both are required to achieve homochirality during Viedma deracemization.[137] They later experimentally elucidated

the importance of attrition and solubility (used to describe the exchange rate of a solute for Ostwald ripening) in generating homochirality.[47]   When they investigated the effects of attrition, they noted that the degree of attrition is affected by many factors such as grinding agent, grinding speed and hardness of the crystal.[52]   When increasing the amount of grinding media or the stirring speed, the probability of attrition is higher and a smaller crystal size distribution is generated.[58] Furthermore, several authors have observed an increase in the rate constant when increasing the amount of stirring media.[47,58,61]   Recently, Blackmond *et al*. suggested that crystal size induced solubility also plays a role in the amplification towards homochirality.[58]   When crystals do not fragment to a certain size during the attrition process, inhibition of the rate of amplification can occur.   Since smaller crystals dissolve more readily then larger crystals, a mixture with a smaller crystal size distribution will more likely undergo Ostwald ripening which was recently demonstrated using isotopic labelled crystals in the amplification of Clopidogrel.[58] While crystal hardness (which affects the attrition probability) was not investigated in this work, it likely plays a central role in fragmentation probability and could explain the different amplification rates obtained for the 5 systems that were investigated.[52,58]

When Noorduin *et al.* investigated the effect of solubility, it was found that the Ostwald ripening probability strongly depended on the exchange rate frequency between solute and crystals (*i.e.* it is dependent on the surface energy of the crystal).[52]   A logarithmic relationship between solubility and crystal surface energy was demonstrated by Nielsen *et al.* using heavy metal salts in aqueous environments.[138] This relationship is in agreement with Noorduin *et al.*'s observation that there is an increase in the rate of amplification with increasing solubility.[47] Given that each of our systems have different solubilities in their respective solvents (Table 5), the rate of Ostwald ripening will also vary from one system to the next.   Consequently, even

though each system underwent asymmetric amplification under similar conditions, they will not all amplify at similar rates due to the variability of the properties stated above.

The amplification time of the Viedma deracemization process has been observed to be influenced by scalemic starting material.[12] For example, a 5% enantiomeric imbalance of sodium chlorate amplifies to homochirality in *ca.* 8 hours in comparison to 24 hours when starting from a racemic mixture. Therefore, the true amplification time for butylated hydroxytoluene is likely longer than what was observed since the starting material had *ca.* 20% enantiomeric excess.

A similar situation occurs for benzophenone since the stirring speed was higher in comparison to the other systems (*i.e.* 3600 rpm *vs.* 2400 rpm). As demonstrated by Viedma, Noorduin *et al.*, and Blackmond *et al.*, the attrition probability increases with increasing the stirring speed.[12,52,58] Therefore, the amplification time for benzophenone should be longer under stirring conditions of 2400 rpm compared to 3600 rpm.

The asymmetric amplification for each system was attempted several times to verify reproducibility and to investigate the asymmetric amplification ratio. For both benzil and diphenyl disulfide, the amplification ratio seems to favor a non-stochastic asymmetric amplification. Since one stock racemic mixture was generated for each system, a potential imbalance may be present. Each of the molecular system stocks was perceived to be racemic by circular dichroism. However, when generating a racemic mixture, it is virtually impossible to begin with a truly racemic initial state with regards to both quantity and particle size.[60] This could explain why the asymmetric amplification ratios were non-stochastic. In the case of diphenyl disulfide, three racemic stocks were made and different amounts of the three stocks, totaling to 0.25 g, were subjected to Viedma deracemization generating a more random ratio compared to benzil.

3.2.Viedma deracemization process by shaking

The attrition process required for Viedma deracemization is typically achieved *via* stirring in the presence of grinding media. However, Viedma deracemization can also be carried out with shaking,[61] sonication,[58] or boiling.[139] In this work, Viedma deracemization was investigated using a high-speed shaking instrument. Taking advantage of the fast amplification times of benzil, shaking conditions for Viedma deracemization were optimized and liquid assisted conditions were examined for this system. Analysis was carried out using the generated calibration curves discussed in section 3.1.2 (Figure 20).

3.2.1. Optimization

Initial optimization consisted of finding an appropriate saturated solvent volume to solid powder ratio. This study resembles the work done by Jones *et al.* where the role of solvent in mechanochemistry was investigated.[76] In this study, an optimization of a refined η parameter ($\eta*$ Equation 3) using saturated solution, rather than solvent, was carried out to find the ideal ratio for asymmetric amplification towards homochirality.

$$\boldsymbol{\eta}^* = \frac{\boldsymbol{Saturated\ solvent\ (\mu L)}}{\boldsymbol{Racemic\ solid\ powder\ (mg)}} \qquad \text{(Equation 3)}$$

At a high $\eta*$ parameter, complete dissolution of the racemic powder takes place after several minutes due to the increase in temperature caused by the friction of the beads when shaking at high speed. Complete dissolution of the chiral crystals is unacceptable, as it will eliminate any chiral amplification achieved up to that point. As the solution subsequently cools, stochastic primary nucleation is expected to give a racemic mixture. When lowering the $\eta*$ parameter, complete dissolution can be avoided. In addition, due to a limitation of the shaking instrument used, 50 seconds of shaking is followed by a 5 minute cooling period. This cooling period allows the sample to cool to room temperature and lowers the probability of complete

dissolution. A ratio of $\eta* = 2$ µL mg^{-1} (400 µL of saturated solvent and 200 mg of racemic powder) was used to obtain the best results (*N.B.* after *ca. 3* minutes [three 50 second shakes] the solid benzil did not completely dissolve) and is ideal for the Viedma deracemization process.

3.2.2. Amplification time

A series of shake cycles (50 seconds of shaking with 5 minutes cooling periods) were used to amplify benzil to homochirality at $\eta* = 2$ µL mg^{-1} (200 mg of racemic powder) (Figure 30). Chiral amplification to *ca.* 20% enantiomeric excess was observed after 250 seconds of shaking (5 cycles). After 500 seconds (10 cycles), amplification to homochirality was achieved (*ca.* 100 % enantiomeric excess). After 750 seconds of shaking (15 cycles), the enantiomeric excess remained at *ca.* 100% as expected. A second stock of racemic powder starting material (used as a control) also amplified to homochirality after 500 seconds. The obtained results are in agreement with the Viedma deracemization process.
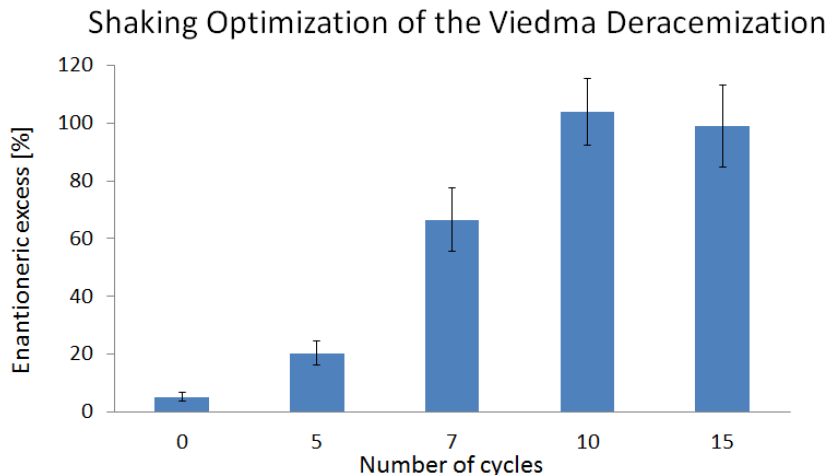

Figure 30. Optimization of Viedma deracemization shaking experiment. A cycle consists of a 50 sec shaking period and 5 min cooling period

3.2.3. Liquid assisted grinding optimization

Different $\eta*$ parameters were investigated to observe the effects of grinding a solid powder at different volumes of saturated solution. Amplification towards homochirality was

achieved when $\eta^* = 2$ or 1 μL mg^{-1} (with 200 mg of solid powder). However, when lowering the

η^* parameter (from 1 to 0.125 μL mg^{-1}) a decrease in the enantiomeric excess was observed

(Figure 31). A similar trend was observed in the work done by Jones *et al.* when forming

different co-crystals under liquid assisted grinding.[76] When they decreased their η parameter, a

decrease in co-crystal formation was observed. The solvent was believed to act as a catalyst to

push the reaction forward. Therefore, it is possible that there is a similar relationship between

the η^* parameter and amplification to homochirality since a decrease in amplification was

observed. However, in this case, the relationship would be based on the amount of contact

between the solid and the solution phase since dissolution to an achiral state is required to

generate a link between enantiomorphic crystals.
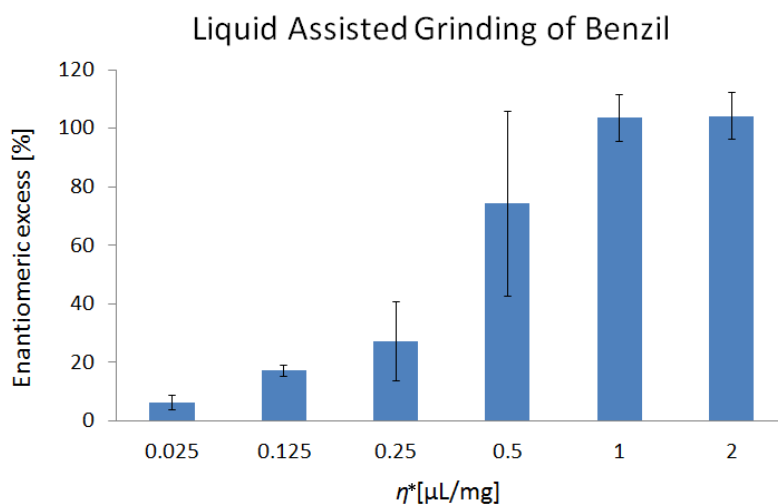
Figure 31. Liquid assisted grinding conditions of the Viedma deracemization process by shaking. All systems under went 20 cycles of shaking (50 seconds of shaking with 5 min cooling periods)

A source of low enantiomeric excess at a low η^* parameter might also be caused by the

loss of solvent through evaporation due to the elevated temperatures that can be reached

during the shaking process.[75] For experiments that use a small amount of solvent, (25 μL and 5

μL corresponding to η^* values of *ca.* 0.25 to 0.025 μL mg^{-1}) the elevated temperature can cause

evaporation and the solvent could escape since the eppendorf lids are not hermetically sealed. Without solution, amplification cannot occur.

Another possibility of the low enantiomeric excess at low η parameter may be caused by the inhibition of attrition. For systems with a small η^* values (0.5 to 0.025 µL mg^{-1}) attrition becomes inhibited by either the powder getting trapped underneath the eppendorf lid or adhering to the surfaces of the eppendorf tubes as a paste. Attrition was proven to be an important driving force in the Viedma deracemization process and without attrition, asymmetric amplification cannot occur.[58]

More work is required to optimize the Viedma deracemization by liquid assisted grinding to achieve homochirality. It is likely that more time is required to reach complete amplification to homochirality. Using a ball mill for these studies may also work more effectively than a cell homogenizer instrument.

3.3. Directed asymmetric amplification

There are several studies that have investigated the potential of directing asymmetric amplification as described in section 1.7.1.[28,62,85,86] In our laboratory, directing the asymmetric amplification of ethylenediammonium sulfate was carried out using a series of amino acids as chiral additives.[85] Interestingly, it was found that the chiral additives could be separated into three distinct categories when directing the asymmetric amplification as described in section 1.7.1. In this work, it was demonstrated that the directing properties of the chiral additives overpowers the starting scalemic mixture of 5% enantiomeric excess during the Viedma deracemization process. Currently, computational modeling is being conducted to investigate the enantioselective adsorption energy of the series of amino acids on enantiomorphic crystal faces of ethylenediammonium sulfate. These computational studies will help propose a

mechanism for chiral additive adsorption on different crystal faces and help rationalize the rule of reversal phenomenon. In this thesis, we further the study of directed asymmetric amplification using racemic benzil mixtures coupled with methylbenzylamine or *cis*-1-amino-2-indanol as chiral additives.

Four different racemic stock powders (A-D) were amplified to homochirality as controls to test the asymmetric amplification without additives. Of the four racemic powders, three (A, B and D) were amplified towards the P-form (Figure 32) and one (C) amplified towards the M-form. It is important to note that for three of the four stock powders (A, B and D), amplification towards only one direction was observed, probably due to some starting imbalance. There was not enough racemic powder in stock C to reproduce the control experiment, so there was not enough data to draw a conclusion on the possible imbalance in this stock.

Asymmetric Amplification of Benzil
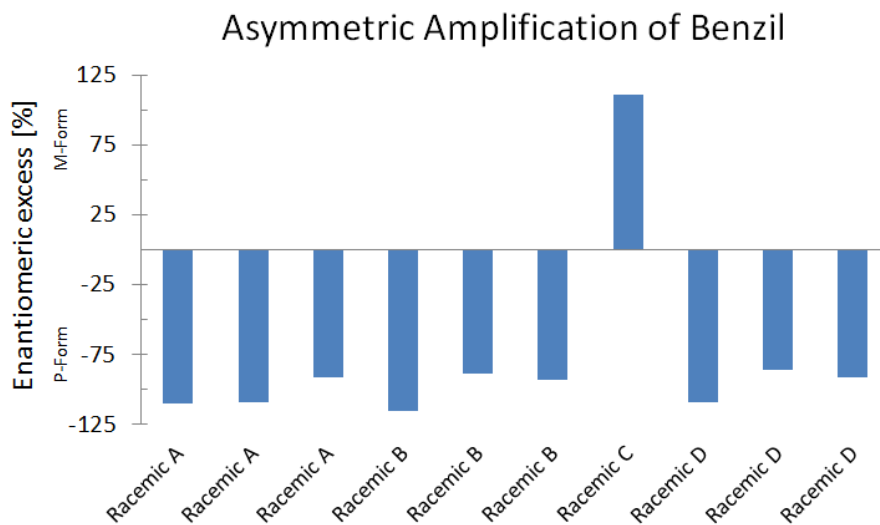
Figure 32. Asymmetric amplification of benzil without additives (as a control – 20 shake cycle)

When incorporating chiral additives in the asymmetric amplification of benzil, directing properties were observed using either (R)- or (S)-methylbenzylamine. However, none were observed using cis-1-amino-2-indanol. The (R)-methylbenzylamine amplified the chirality towards M-form benzyl (9 times out of 11) and the (S)-methylbenzylamine amplified the

chirality towards P-form benzil (11 times out of 11) (Figure 34). This can be rationalized using Addadi *et al.'s* rule of reversal,[87] where they investigated the potential of separating stochastic crystallization of conglomerate systems using chiral additives as described in section 1.7.1. The same idea can be applied when using the Viedma deracemization process in the presence of chiral additives. An enantiopure chiral additive may have the ability to enantioslectively adsorb on the surface of a crystal and inhibit its growth or affects dissolution. Since the chiral additive adsorbs to the surface, it inhibits the molecule's ability to pack efficiently during crystal growth (secondary crystallization).[84] This inhibition of growth has also been observed using enantiopure amino acids on crystals of asparagine[140] and calcite.[84] This imbalance, caused by the addition of chiral additives, will drive the Viedma deracemization process to feed the faster crystallizing enantiomorph (Figure 34).
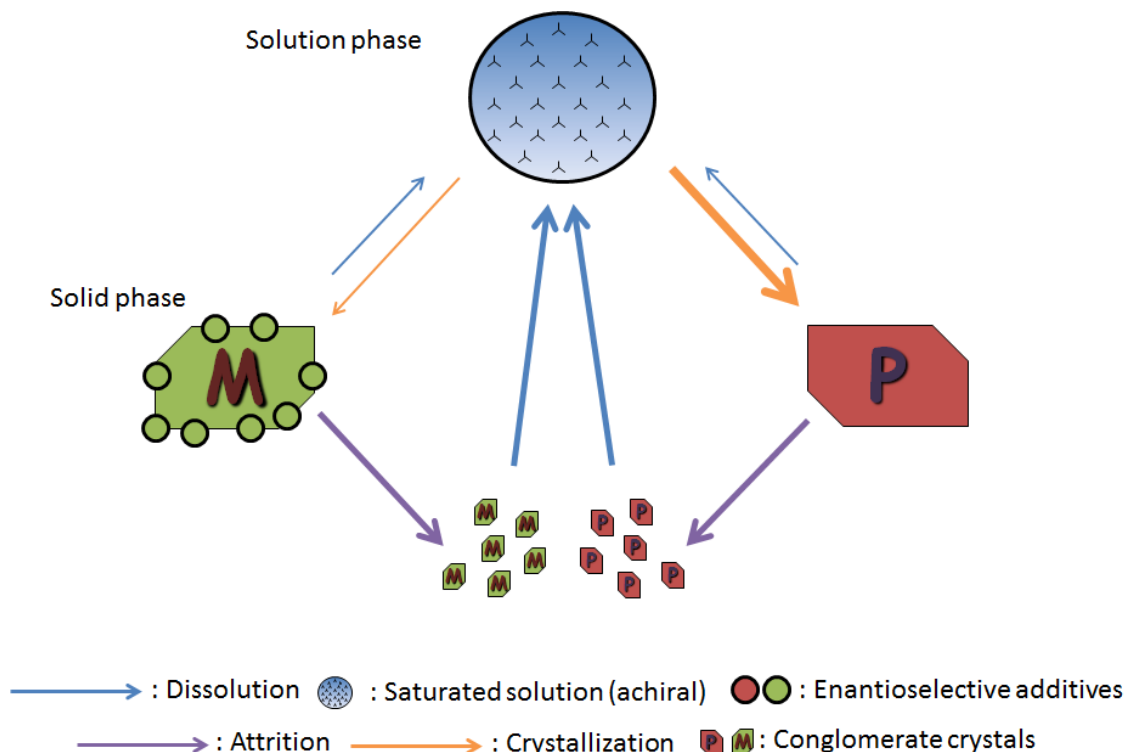

Figure 33. Attrition enhanced Ostwald ripening mechanism with a chiral additive: Crystallization (orange arrow) occurs more readily to the P-form crystal since the chiral additive enantioselectively adsorbs on the M-form crystal inhibiting its growth

We propose, by Adaddi's rule of reversal, that the amplification towards the M-form of benzil is caused by (R)-methylbenzylamine interacting with the P-form benzil crystal (Figure 34). The opposite can be said for the (S)-methylbenzylamine amplification to the P-form benzil crystal. It is believed that the additive interacts with the chiral crystals *via* an enantiospecific nonlinear three point contact process as described in section 1.7.1.[80] The 2 out of 11 times where (R)-methylbenzylamine directed the asymmetric amplification towards P-form benzil could be explained by looking at the control experiment. Both racemic mixtures B and D always amplified towards P-form benzil and it is possible that the imbalance present in both starting mixtures had a stronger influence than the chiral additive. Therefore, the asymmetric amplification was overpowered by the initial imbalance and was not affected by the methylbenzylamine additive. The same phenomenon could also explain why no directing properties were observed for the cis-1-amino-2-indanol. However, additional investigations are required to understand why this chiral additive did not direct the asymmetric amplification and no firm conclusions can be made.
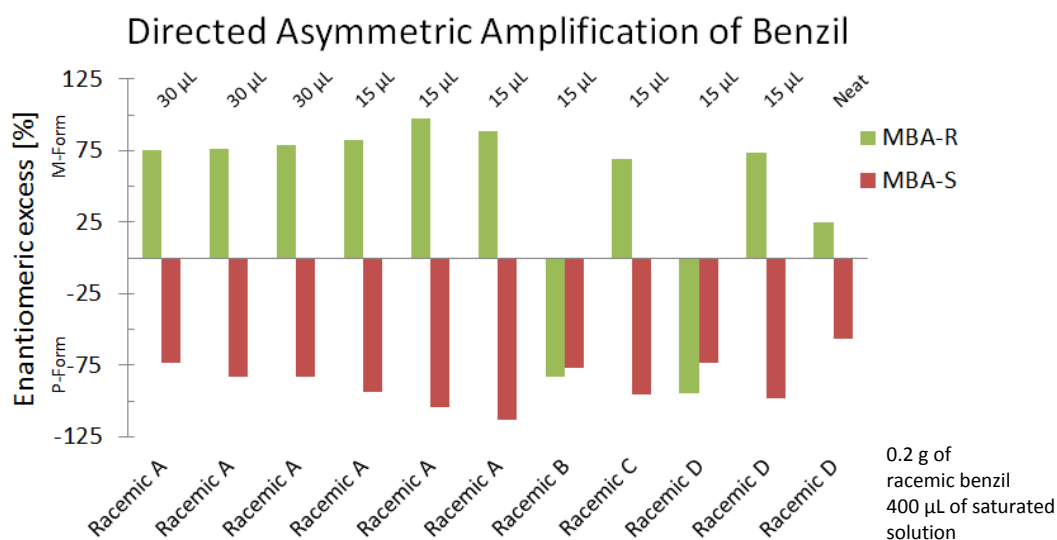

Figure 34. Directed chiral amplification of benzil using (R) or (S)-methylbenzylamine as an additive: Volumes represent how much (R) or (S)-methylbenzylamine was added to the saturated solution and neat represents doing the experiment in saturated (R) or (S)-methylbenzylamine (20 shake cycles)

Different amounts of (R) or (S)-methylbenzylamine were investigated to find the limiting volume needed to direct the asymmetric amplification. Using different volumes of methylbenzylamine also affected the enantiomeric excess obtained. When using 30 µL of methylbenzylamine, an enantiomeric excess of *ca.* 75% was observed after 17 minutes of shaking (20 cycles). This may be due to excess methylbenzylamine trapped in the benzil powder matrix as the solid appeared to be waxy. The methylbenzylamine trapped in the matrix would generate a lower circular dichroism value as the benzil concentration is lower compared to a pure sample of similar weight. A minimum of 15 µL was required to direct the asymmetric amplification. However, directed amplification did not always occur at this volume possibly due to the overpowering imbalance effects of the starting material as stated above. At 15 µL, very little methylbenzylamine appeared to be trapped in the powder matrix and enantiomeric excess values of *ca.* 85% were obtained.

To validate the directing properties of methylbenzylamine, a saturated methylbenzylamine (neat) solution was used instead of adding the additive in saturated acetone. Using a methylbenzylamine solution, an amplification of *ca.* 25% was obtained with (R)-methylbenzylamine directing towards M-form benzil and an amplification of *ca*. 50% was obtained with (S)-methylbenzylamine directing towards P-form benzil after 20 cycles. The low percent enantiomeric excess can be explained by the change of dissolution and crystallization rates since these experiments were carried out with a different solvent with different ability to solubilize benzil.[52] Given more shaking time, there is a good probability that the saturated (R)-methylbenzylamine would direct the asymmetric amplification towards homochiral M-form benzil and saturated (S)-methylbenzylamine would direct the asymmetric amplification towards homochiral P-form benzil.

4. Conclusion

In this investigation, the chiral crystallization distribution and the generality of the Viedma deracemization process were established for five achiral conglomerate systems. For every system, except benzil, a non-stochastic crystallization distribution was observed and was possibly governed by a cryptochiral environment. These results demonstrated the sensitivity of chiral crystallization and the difficulties of obtaining a stochastic ratio. Non-stochastic chiral crystallization in conglomerate systems has been observed previously and it should be noted that, "other examples of this phenomenon may indeed exist, although they are prone to scorn from journal referees, as the processes are nigh on impossible to explain in a rational manner, especially when only one enantiomer is repeatedly produced".[141] It can be as simple as the starting material used for crystallization being scalemic rather than racemic, as is often assumed. For example, the reason we prepared our own racemic mixtures was because commercial benzil (37.01% *ee* towards the M-form), diphenyl disulfide (33.90% *ee* towards the P-form), benzophenone (30.64% *ee* towards the P-form), butylated hydroxytoluene (50.00% *ee* towards the left-handedness) and tetraphenylethyelne (6.10 % *ee* towards the left-handedness) were all scalemic. These 5 achiral molecular systems were the first organic molecules to undergo asymmetric amplification in organic solvent based on an attrition-enhanced Ostwald ripening mechanism. Each of the 5 systems reached homochirality under similar conditions: (*i*) 2 hours for benzil, (*ii*) 8 hours for diphenyl disulfide, (*iii*) 24 hours for benzophenone, (*iv*) 26 hours for butylated hydroxytoluene and (*v*) 30 hours for tetraphenylethylene, which all fall within the time frame of the literature achiral systems.[12,51,61] This corroborates the validity of achiral conglomerate system amplification to homochirality *via* the Viedma deracemization process. In addition, these five achiral molecules can now be added to the list of 13 molecules that have been shown to undergo asymmetric amplification *via* the Viedma deracemization process.

Future work will be to investigate other novel systems that may undergo asymmetric amplification. Taking advantage of the naturally interconverting systems such as atropisomers, co-crystals and valence isomers, can give further insights on the driving force, mechanism and validity of this process. Some of the molecules that can be investigated are tri-*o*-thymotide (atropisomer),[142] 3-azabicyclo[3.3.1]nonane system (atropisomers),[143] chiral catenanes (architectural atropisomer),[144] pyrimidinone (atropisomer),[145] pyrimidinethione (atropisomer),[145] and a cyclooctatetraene dimer (valence isomer).[146]

Taking advantage of the fast amplification rates of racemic solid benzil mixtures, a shaking mechanism and liquid assisted grinding conditions were investigated and, after optimization, yielded homochirality. The optimized saturated solvent to solid ratio was established to be 2 μL mg^{-1} and amplification towards homochirality was observed with a ratio as low as 0.125 μL mg^{-1}. This work demonstrated that the asymmetric amplification could be accomplished very quickly (*i.e.* 10 minutes) under optimized shaking conditions. The results obtained from the liquid assisted grinding experiments give us further insight that very little saturated solvent is required to asymmetrically amplify a racemic mixture to homochirality. Such liquid assisted grinding conditions may have potential in the pharmaceutical industry. One of our future goals is to attempt asymmetric amplification using sublimation conditions rather than a saturated solvent. Under sublimation conditions, molecules in the vapor phase will have the ability to racemize and may allow asymmetric amplification to take place. Based on our liquid assisted grinding results, equilibrium between the vapor phase and solid phase may be all that is required for successful Viedma deracemization.

Lastly, directing the asymmetric amplification of racemic benzil was achieved using either (R) or (S)-methylbenzylamine as a chiral additive. The (R)-methylbenzylamine

asymmetrically amplified the benzil towards the M-form 9 out of 11 times and the (S)-methylbenzylamine asymmetrically the benzil towards the P-form 11 out of 11 times. Future work on understanding the selective adsorption of methylbenzylamine on the surface of benzil will be investigated using both a theoretical and experimental approach. The interaction energy difference between chiral additives and crystalline surface can be computationally calculated and experimentally examined. Experimental method such as atomic force microscopy, surface etching and crystallization under the influence of chiral additives can be used to shed light on these critical interactions.

To conclude, this work has shed light on the process of Viedma deracemization as a means for the asymmetric amplification of racemic mixture, contributing towards a better understanding of the origins of homochirality. Indeed a recent report implicating a conglomerate crystal amplification process in the Tagish Lake meteorite, "provides support for the hypothesis that significant enantiomeric enrichments for some amino acids could form by abiotic processes prior to the emergence of life".[147] Furthermore, this work demonstrated the strength of using solid-state circular dichroism as a method to analyze chiral samples and monitoring the Viedma deracemization process with time.

5. References

(1)   Blackmond, D. G. *Cold Spring Harb. Perspect. Biol.* **2010**, *2*, 1.

(2)   Avalos, M.; Babiano, R.; Cintas, P.; Jimenez, J. L.; Palacios, J. C. *Tetrahedron: Asymmetry* **2010**, *21*, 1030.

(3)   Meinert, C.; Filippi, J.-J.; Nahon, L.; Hoffmann, S. V.; d'Hendecourt, L.; de, M. P.; Bredehoft, J. H.; Thiemann, W. H. P.; Meierhenrich, U. J. *Symmetry* **2010**, *2*, 1055.

(4)   Toxvaerd, S. *Int. J. Mol. Sci.* **2009**, *10*, 1290.

(5)   Elitzur, A. C.; Shinitzky, M. *Los Alamos Natl. Lab., Prepr. Arch., Phys.* **2006**, 1.

(6)   Guijarro, A.; Yus, M. *The Origin of Chirality in the Molecules of Life*; RCS Publishing: Cambridge, 2009.

(7)   Frank, F. C. *Biochim. Biophys. Acta* **1953**, *11*, 459.

(8)   Cartwright, J. H. E.; Piro, O.; Tuval, I. *Phys. Rev. Lett.* **2007**, *98*, 165501/1.

(9)   Cairns-Smith, A. G. *Chem. Br.* **1986**, *22*, 559.

(10)   Cintas, P. *Angew. Chem., Int. Ed.* **2008**, *47*, 2918.

(11)   Kojo, S.; Tanaka, K. *Chem. Commun.* **2001**, 1980.

(12)   Viedma, C. *Phys. Rev. Lett.* **2005**, *94*, 065504/1.

(13)   Dryzun, C.; Avnir, D. *Chem. Commun.* **2012**, *48*, 5874.

(14)   Flack, H. D. *Helv. Chim. Acta* **2003**, *86*, 905.

(15)   Flack, H. D. *Acta Crystallogr., Sect. A: Found. Crystallogr.* **2009**, *A65*, 371.

(16)   Suh, I. I. H.; Park, K. H.; Jensen, W. P.; Lewis, D. E. *J. Chem. Educ.* **1997**, *74*, 800.

(17)   LaPlante, S. R.; Fader, L. D.; Fandrick, K. R.; Fandrick, D. R.; Hucke, O.; Kemper, R.; Miller, S. P. F.; Edwards, P. J. *J. Med. Chem.* **2011**, *54*, 7005.

(18)   Mellin, G. W.; Katzenstein, M. *N. Engl. J. Med.* **1962**, *267*, 1184.

(19)   Williams, A. *Pestic. Sci.* **1996**, *46*, 3.

(20)   Garcia-Canas, V.; Cifuentes, A. *Electrophoresis* **2008**, *29*, 294.

(21)   Ward, T. J.; Ward, K. D. *Anal. Chem.* **2012**, *84*, 626.

(22)   Satyanarayana, T.; Abraham, S.; Kagan, H. B. *Angew. Chem., Int. Ed.* **2009**, *48*, 456.

(23)   Wang, J.; Peng, Q.; Li, G. *Afr. J. Biotechnol.* **2009**, *8*, 4299.

(24)   Rekoske, J. E. *AIChE J.* **2001**, *47*, 2.

(25)   Jacques, J.; Collet, A.; Wilen, S. H. *Enantiomers, racemates, and resolutions*; John Wiley & Sons, Inc.: New-York, 1981.

(26)   Galland, A.; Dupray, V.; Berton, B.; Morin-Grognet, S.; Sanselme, M.; Atmani, H.; Coquerel, G. *Cryst. Growth Des.* **2009**, *9*, 2713.

(27)   Havinga, E. *Biochim. Biophys. Acta* **1954**, *13*, 171.

(28)   Noorduin, W. L.; Izumi, T.; Millemaggi, A.; Leeman, M.; Meekes, H.; Van, E. W. J. P.; Kellogg, R. M.; Kaptein, B.; Vlieg, E.; Blackmond, D. G. *J. Am. Chem. Soc.* **2008**, *130*, 1158.

(29)   Seeber, G.; Tiedemann, B. E. F.; Raymond, K. N. *Top. Curr. Chem.* **2006**, *265*, 147.

(30)   Mateos-Timoneda, M. A.; Crego-Calama, M.; Reinhoudt, D. N. *Chem. Soc. Rev.* **2004**, *33*, 363.

(31)   Grzybowski, B. A.; Wilmer, C. E.; Kim, J.; Browne, K. P.; Bishop, K. J. M. *Soft Matter* **2009**, *5*, 1110.

(32)   Whitesides, G. M.; Grzybowski, B. *Science* **2002**, *295*, 2418.

(33)   Dhanaraj, G.; Byrappa, K.; Prasad, V.; Dudley, M. *Springer Handbook of Crystal Growth*; Springer-Verlag Berlin Heidelberg: New York, 2010.

(34)   Mullin, J. W. *Crystallization*; 4th ed.; Reed Educational and Professional Publishing LTD: Oxford, 2001.

(35) Tilley, R. *Crystals and Crystal Structures*; John Wiley & Sons, LTD: West Sussex, 2006.

(36) Hall, S.; McMahon, B. *International Tables for Crystallography: Definitions and Exchange on Crystallographic Data*; 1st ed.; Springner: The Netherlands, 2005; Vol. G.

(37) Massa, W. *Crystal Structure Determination*; 2nd ed.; Springer: New York, 2004.

(38) Burckhardt, J. J. *Arch. Hist. Exact. Sci.* **1967**, *4*, 235.

(39) Weng, N. S.; Hu, S.-Z. *Jiegou Huaxue* **2003**, *22*, 37.

(40) Matsuura, T.; Koshima, H. *J. Photochem. Photobiol., C* **2005**, *6*, 7.

(41) Brock, C. P.; Schweizer, W. B.; Dunitz, J. D. *J. Am. Chem. Soc.* **1991**, *113*, 9811.

(42) Kipping, F. S.; Pope, W. J. *Nature* **1898**, *59*, 53.

(43) Kondepudi, D. K.; Kaufman, R. J.; Singh, N. *Science* **1990**, *250*, 975.

(44) Kondepudi, D. K.; Laudadio, J.; Asakura, K. *J. Am. Chem. Soc.* **1999**, *121*, 1448.

(45) Sainz-Diaz, C. I.; Martin-Islan, A. P.; Cartwright, J. H. E. *J. Phys. Chem. B* **2005**, *109*, 18758.

(46) Meekes, H.; Noorduin, W. L.; Kaptein, B.; Kellogg, R. M.; Deroover, G.; van, E. W. J.; Vlieg, E.; American Chemical Society: 2011, p I+EC.

(47) Noorduin, W. L.; Meekes, H.; van, E. W. J. P.; Millemaggi, A.; Leeman, M.; Kaptein, B.; Kellogg, R. M.; Vlieg, E. *Angew. Chem., Int. Ed.* **2008**, *47*, 6445.

(48) Iggland, M.; Mazzotti, M. *Cryst. Growth Des.* **2012**, *12*, 1489.

(49) Skrdla, P. J. *Cryst. Growth Des.* **2011**, *11*, 1957.

(50) Uwaha, M. *J. Phys. Soc. Jpn.* **2008**, *77*, 083802/1.

(51) Viedma, C. *Astrobiology* **2007**, *7*, 312.

(52) Noorduin, W. L.; van, E. W. J. P.; Meekes, H.; Kaptein, B.; Kellogg, R. M.; Tully, J. C.; McBride, J. M.; Vlieg, E. *Angew. Chem., Int. Ed.* **2010**, *49*, 8435.

(53) Uwaha, M. *J. Phys. Soc. Jpn.* **2004**, *73*, 2601.

(54) Noorduin, W. L.; Vlieg, E.; Kellogg, R. M.; Kaptein, B. *Angew. Chem., Int. Ed.* **2009**, *48*, 9600.

(55) Leisegang, R. E. *Zeitschrift für Physikalische Chemie* **1911**, *75*, 374.

(56) Crusats, J.; Veintemillas-Verdaguer, S.; Ribo, J. M. *Chem. Eur. J.* **2006**, *12*, 7776.

(57) Blackmond, D. G. *Chem. Eur. J.* **2007**, *13*, 3290.

(58) Hein, J. E.; Cao, B. H.; Viedma, C.; Kellogg, R. M.; Blackmond, D. G. *J. Am. Chem. Soc.* **2012**, *134*, 12629.

(59) Viedma, C. *Cryst. Growth Des.* **2007**, *7*, 553.

(60) Siegel, J. S. *Chirality* **1998**, *10*, 24.

(61) Cheung, P. S. M.; Gagnon, J.; Surprenant, J.; Tao, Y.; Xu, H.; Cuccia, L. A. *Chem. Commun.* **2008**, 987.

(62) Leeman, M.; Noorduin, W. L.; Millemaggi, A.; Vlieg, E.; Meekes, H.; van, E. W. J. P.; Kaptein, B.; Kellogg, R. M. *CrystEngComm* **2010**, *12*, 2051.

(63) Kaptein, B.; Noorduin, W. L.; Meekes, H.; van, E. W. J. P.; Kellogg, R. M.; Vlieg, E. *Angew. Chem., Int. Ed.* **2008**, *47*, 7226.

(64) Levilain, G.; Rougeot, C.; Guillen, F.; Plaquevent, J.-C.; Coquerel, G. *Tetrahedron: Asymmetry* **2009**, *20*, 2769.

(65) Viedma, C.; Ortiz, J. E.; de, T. T.; Izumi, T.; Blackmond, D. G. *J. Am. Chem. Soc.* **2008**, *130*, 15274.

(66) Rybak, W. K. *Tetrahedron: Asymmetry* **2008**, *19*, 2234.

(67) Noorduin, W. L.; van, d. A. P.; Bode, A. A. C.; Meekes, H.; van, E. W. J. P.; Vlieg, E.; Kaptein, B.; van, d. M. M. W.; Kellogg, R. M.; Deroover, G. *Org. Process Res. Dev.* **2010**, *14*, 908.

(68) Noorduin, W. L.; Kaptein, B.; Meekes, H.; van, E. W. J. P.; Kellogg, R. M.; Vlieg, E. *Angew. Chem., Int. Ed.* **2009**, *48*, 4581.

(69) Arai, K.; Ohara, Y.; Takakuwa, Y.; Iizumi, T.; Nissan Chemical Industries, Ltd., Japan . 1983, p 5 pp.

(70) Flock, A. M.; Reucher, C. M. M.; Bolm, C. *Chem. Eur. J.* **2010**, *16*, 3918.

(71) Tsogoeva, S. B.; Wei, S.; Freund, M.; Mauksch, M. *Angew. Chem., Int. Ed.* **2009**, *48*, 590.

(72) Friscic, T. *J. Mater. Chem.* **2010**, *20*, 7599.

(73) Toda, F.; Schmeyers, J. *Green Chem.* **2003**, *5*, 701.

(74) Garay, A. L.; Pichon, A.; James, S. L. *Chem. Soc. Rev.* **2007**, *36*, 846.

(75) Friscic, T.; Jones, W. *Cryst. Growth Des.* **2009**, *9*, 1621.

(76) Friscic, T.; Childs, S. L.; Rizvi, S. A. A.; Jones, W. *CrystEngComm* **2009**, *11*, 418.

(77) Shan, N.; Toda, F.; Jones, W. *Chem. Commun.* **2002**, 2372.

(78) Schmidt, R.; Stolle, A.; Ondruschka, B. *Green Chem.* **2012**, *14*, 1673.

(79) Lee, T.; Tsai, M. H.; Lee, H. L. *Cryst. Growth Des.* **2012**, *12*, 3181.

(80) Hazen, R. M.; Sholl, D. S. *Nat. Mater.* **2003**, *2*, 367.

(81) Hazen, R. M.; Filley, T. R.; Goodfriend, G. A. *Proc. Natl. Acad. Sci. U. S. A.* **2001**, *98*, 5487.

(82) Kuhnle, A.; Linderoth, T. R.; Hammer, B.; Besenbacher, F. *Nature* **2002**, *415*, 891.

(83) Huang, Y.; Gellman, A. J. *Top. Catal.* **2011**, *54*, 1403.

(84) Orme, C. A.; Noy, A.; Wierzbicki, A.; McBride, M. T.; Grantham, M.; Teng, H. H.; Dove, P. M.; DeYoreo, J. J. *Nature* **2001**, *411*, 775.

(85) Cheung, P. S. M.; Cuccia, L. A. *Chem. Commun.* **2009**, 1337.

(86) Noorduin, W. L.; van, d. A. P.; Meekes, H.; van, E. W. J. P.; Kaptein, B.; Leeman, M.; Kellogg, R. M.; Vlieg, E. *Angew. Chem., Int. Ed.* **2009**, *48*, 3278.

(87) Addadi, L.; Weinstein, S.; Gati, E.; Weissbuch, I.; Lahav, M. *J. Am. Chem. Soc.* **1982**, *104*, 4610.

(88) Noorduin, W. L.; Bode, A. A. C.; van, d. M. M.; Meekes, H.; van, E. A. F.; van, E. W. J. P.; Christianen, P. C. M.; Kaptein, B.; Kellogg, R. M.; Rasing, T.; Vlieg, E. *Nat. Chem.* **2009**, *1*, 729.

(89) Zill, D. G.; Wright, W. S.; Cullen, M. R. *Advanced Engineering Mathematics*; 4th ed.; Jones and Bartlett Publishers 2011.

(90) Pincock, R. E.; Perkins, R. R.; Ma, A. S.; Wilson, K. R. *Science* **1971**, *174*, 1018.

(91) Wald, G. *Ann. N. Y. Acad. Sci.* **1957**, *69*, 352.

(92) Vestergren, M.; Johansson, A.; Lennartson, A.; Hakansson, M. *Mendeleev Commun.* **2004**, 258.

(93) Riha, J.; Vysin, I.; Lapsanska, H. *Mol. Cryst. Liq. Cryst.* **2005**, *442*, 181.

(94) Kosa, C.; Lukac, I.; Weiss, R. G. *Macromol. Chem. Phys.* **1999**, *200*, 1080.

(95) Brown, C. J.; Sadanaga, R. *Acta Crystallogr.* **1965**, *18*, 158.

(96) Lumbroso, H.; Catel, J. M.; Le, C. G.; Andrieu, C. G. *J. Mol. Struct.* **1999**, *513*, 201.

(97) Lee, J. D.; Bryant, M. W. R. *Acta Crystallogr., Sect. B: Struct. Sci.* **1969**, *B25*, 2094.

(98) Chin, K. K.; Natarajan, A.; Gard, M. N.; Campos, L. M.; Shepherd, H.; Johansson, E.; Garcia-Garibay, M. A. *Chem. Commun.* **2007**, 4266.

(99) Szyrszyng, M.; Nowak, E.; Gdaniec, M.; Milewska, M. J.; Polonski, T. *Tetrahedron: Asymmetry* **2004**, *15*, 103.

(100) Fleischer, E. B.; Sung, N.; Hawkinson, S. *J. Phys. Chem.* **1968**, *72*, 4311.

(101) Brewer, M. S. *Compr. Rev. Food Sci. Food Saf.* **2011**, *10*, 221.

(102) Maze-Baudet, M. *Acta Crystallogr., Sect. B: Struct. Sci.* **1973**, *29*, 602.

(103) Jana, D.; Ghorai, B. K. *Tetrahedron Lett.* **2012**, *53*, 196.

(104) Hoekstra, A.; Vos, A. *Acta Crystallogr., Sect. B: Struct. Sci.* **1975**, *B31*, 1716.

(105) Wang, J.-R.; Carbone, M.; Gavagnin, M.; Mandi, A.; Antus, S.; Yao, L.-G.; Cimino, G.; Kurtan, T.; Guo, Y.-W. *Eur. J. Org. Chem.* **2012**, *2012*, 1107.

(106) Han, Z.-B.; Ji, J.-W.; An, H.-Y.; Zhang, W.; Han, G.-X.; Zhang, G.-X.; Yang, L.-G. *Dalton Trans.* **2009**, 9807.

(107) Hou, Y.; Fang, X.; Hill, C. L. *Chem. Eur. J.* **2007**, *13*, 9442.

(108) Tan, H.; Li, Y.; Chen, W.; Liu, D.; Su, Z.; Lu, Y.; Wang, E. *Chem. Eur. J.* **2009**, *15*, 10940.

(109) Pucci, A.; Nannizzi, S.; Pescitelli, G.; Di, B. L.; Ruggeri, G. *Macromol. Chem. Phys.* **2004**, *205*, 786.

(110) Nishiguchi, N.; Kinuta, T.; Sato, T.; Nakano, Y.; Harada, T.; Tajima, N.; Fujiki, M.; Kuroda, R.; Matsubara, Y.; Imai, Y. *Cryst. Growth Des.* **2012**, *12*, 1859.

(111) Ou, G.-C.; Jiang, L.; Feng, X.-L.; Lu, T.-B. *Inorg. Chem.* **2008**, *47*, 2710.

(112) Peacock, R. D. *J. Chem. Soc., Dalton Trans.* **1983**, 291.

(113) Geiser, U.; Guedel, H. U. *Inorg. Chem.* **1981**, *20*, 3013.

(114) Olszewska, T.; Gdaniec, M.; Polonski, T. *Tetrahedron: Asymmetry* **2009**, *20*, 1308.

(115) Hou, J.-B.; Tang, G.; Guo, J.-N.; Liu, Y.; Zhang, H.; Zhao, Y.-F. *Tetrahedron: Asymmetry* **2009**, *20*, 1301.

(116) Lin, L.; Yu, R.; Yang, W.; Wu, X.-Y.; Lu, C.-Z. *Cryst. Growth Des.* **2012**, *12*, 3304.

(117) Cui, P.; Ren, L.; Chen, Z.; Hu, H.; Zhao, B.; Shi, W.; Cheng, P. *Inorg. Chem.* **2012**, *51*, 2303.

(118) Polonski, T.; Szyrszyng, M.; Gdaniec, M.; Nowak, E.; Herman, A. *Tetrahedron: Asymmetry* **2001**, *12*, 797.

(119) Kawasaki, T.; Nakaoda, M.; Kaito, N.; Sasagawa, T.; Soai, K. *Origins Life Evol. Biosphere* **2010**, *40*, 65.

(120) Shimizu, T.; Isono, H.; Yasui, M.; Iwasaki, F.; Kamigata, N. *Org. Lett.* **2001**, *3*, 3639.

(121) Yao, Q.-X.; Xuan, W.-M.; Zhang, H.; Tu, C.-Y.; Zhang, J. *Chem. Commun.* **2009**, 59.

(122) Harada, T.; Sato, T.; Kuroda, R. *Chem. Phys. Lett.* **2008**, *456*, 268.

(123) Toyota, S.; Asakura, M.; Oki, M.; Toda, F. *Bull. Chem. Soc. Jpn.* **2000**, *73*, 2357.

(124) Olszewska, T.; Nowak, E.; Gdaniec, M.; Polonski, T. *Org. Lett.* **2012**, *14*, 2568.

(125) Walkiewicz, A. E. Doctor of Philosophy, University of Birmingham, 2010.

(126) Ding, L.; Lin, L.; Liu, C.; Li, H.; Qin, A.; Liu, Y.; Song, L.; Zhang, H.; Tang, B. Z.; Zhao, Y. *New J. Chem.* **2011**, *35*, 1781.

(127) Freund, J. E. *Statistics A first course*; 2nd ed.; Prentice-Hall, Inc: Engelwood Cliffs, New Jersey, 1976.

(128) Osuna-Esteban, S.; Zorzano, M. P.; Menor-Salvan, C.; Ruiz-Bermejo, M.; Veintemillas-Verdaguer, S. *Phys. Rev. Lett.* **2008**, *100*, 146102/1.

(129) Lennartson, A. Doctral Thesis University of Gothenburg, 2009.

(130) Lennartson, A.; Vestergren, M.; Hakansson, M. *Chem. Eur. J.* **2005**, *11*, 1757.

(131) Johansson, A.; Haakansson, M. *Chem. Eur. J.* **2005**, *11*, 5238.

(132) Johansson, A.; Haakansson, M.; Jagner, S. *Chem. Eur. J.* **2005**, *11*, 5311.

(133) Liu, C.-Y.; Yan, J.-X.; Lin, Y.-J.; Li, D.; Fang, X.-M.; Zhang, H. *Wuli Huaxue Xuebao* **2012**, *28*, 257.

(134) Castiglioni, E.; Biscarini, P.; Abbate, S. *Chirality* **2009**, *21*, e28.

(135) Kuroda, R.; Honma, T. *Chirality* **2000**, *12*, 269.

(136) Castiglioni, E.; Abbate, S.; Longhi, G.; Gangemi, R. *Chirality* **2007**, *19*, 491.

(137) Noorduin, W. L.; Meekes, H.; Bode, A. A. C.; van, E. W. J. P.; Kaptein, B.; Kellogg, R. M.; Vlieg, E. *Cryst. Growth Des.* **2008**, *8*, 1675.

(138) Nielsen, A. E.; Sohnel, O. *J. Cryst. Growth* **1971**, *11*, 233.

(139) Viedma, C.; Cintas, P. *Chem. Commun.* **2011**, *47*, 12786.

(140) Shimon, L. J. W.; Lahav, M.; Leiserowitz, L. *J. Am. Chem. Soc.* **1985**, *107*, 3375.

(141) Amabilino, D. B.; Kellogg, R. M. *Isr. J. Chem.* **2011**, *51*, 1034.

(142) Bonner, W. A. *Origins Life Evol. Biosphere* **1999**, *29*, 317.

(143) Olszewska, T.; Milewska, M. J.; Gdaniec, M.; Polonski, T. *Tetrahedron: Asymmetry* **2012**, *23*, 278.

(144) Alcalde, E.; Perez-Garcia, L.; Ramos, S.; Stoddart, J. F.; White, A. J. P.; Williams, D. J. *Mendeleev Commun.* **2004**, 233.

(145) Sakamoto, M.; Yagishita, F.; Ando, M.; Sasahara, Y.; Kamataki, N.; Ohta, M.; Mino, T.; Kasashima, Y.; Fujita, T. *Org. Biomol. Chem.* **2010**, *8*, 5418.

(146) Siegwarth, J.; Bornhoft, J.; Nather, C.; Herges, R. *Org. Lett.* **2009**, *11*, 3450.

(147) Glavin, D. P.; Elsila, J. E.; Burton, A. S.; Callahan, M. P.; Dworkin, J. P.; Hilts, R. W.; Herd, C. D. K. *Meteorit. Planet. Sci.* **2012**, 1.